

# Extended Landauer-Büttiker Formula for Current through Open Quantum Systems with Gain or Loss

Chao Yang<sup>1,2,3</sup> and Yucheng Wang<sup>1,2,3,\*</sup>

<sup>1</sup>*Shenzhen Institute for Quantum Science and Engineering,  
Southern University of Science and Technology, Shenzhen 518055, China*

<sup>2</sup>*International Quantum Academy, Shenzhen 518048, China*

<sup>3</sup>*Guangdong Provincial Key Laboratory of Quantum Science and Engineering,  
Southern University of Science and Technology, Shenzhen 518055, China*

The Landauer-Büttiker formula, which characterizes current through a finite region connected to leads, is a cornerstone in studying transport phenomena. We extend this formula using the Lindblad-Keldysh formalism to describe particle and energy currents in regions with gain or loss. The derived formula shows that gain or loss plays a notable role in shaping the transport properties. Based on this formula, we find that inversion symmetry breaking in the gain and loss terms or in the system can generate current, along with the anomalous phenomenon where disorder induces current. We also reveal how gain and loss affect thermal and electrical conductances, as well as the impact of bond loss-induced non-Hermitian skin effect on current. This work deepens and extends our understanding of transport phenomena in open systems.

*Introduction.*— Studying quantum transport properties is essential for understanding condensed-matter systems and has broad applications, such as in various electronic devices, atomic and photonic technologies, nanotechnology, and quantum computing [1–7]. One of the most influential frameworks for understanding transport is the Landauer-Büttiker formula [8, 9], which expresses current in terms of the system’s transmission coefficient and the electron distribution within connected leads. Beyond electrons, this formalism applies universally to any quantum system—including atomic [10–14], photonic [15, 16], and phononic [17] systems—where transport reduces to a scattering problem with well-defined transmission channels [18]. The system described by this formula, aside from being coupled to two leads, is not influenced by any form of dissipation. However, dissipation is widespread, and understanding its effects on quantum transport is a fundamentally important issue.

With the advancements in experimental techniques for controlling different types of dissipation [19–50], recent years have seen a growing interest in dissipative open quantum systems. While dissipation is typically viewed as detrimental to quantum correlations, recent research has revealed that it can also give rise to novel physical phenomena [22–38, 42–56] or phase transitions [57–68], profoundly impacting dynamics. A common type of dissipation is dephasing, which can reduce coherence, thereby breaking localization and ballistic transport, and inducing diffusive transport [69–81]. Another important type of dissipation is particle gain or loss. This process can arise from a variety of physical mechanisms, such as proximity effects in heterostructures [82–85], uncontrolled leakage in experimental setups [86–88], or engineered coupling in platforms like cold atoms, photonic lattices, superconducting circuits, and ion traps [32–50]. Despite the increasing relevance of the transport properties in such systems [38–46, 89–102], a general transport

formula that uniformly captures the effects of gain and loss has not yet been established. This limits our understanding of their impact on currents and hinders the prediction of novel nonequilibrium phenomena.

In this Letter, we derive a general formula to describe particle and energy currents in systems with arbitrary forms of gain or loss, providing a foundational framework for investigating how gain or loss impacts transport properties. Based on this formula, we reveal several non-trivial transport properties in open systems.

*Model.*— We consider a one-dimensional system coupled to leads at its ends and exchanging particles with Markovian reservoirs (see Fig. 1). After tracing out the reservoirs, their effects are captured by gain/loss terms in the Lindblad master equation [2, 88, 103–106, 108] (see Supplemental Materials [108] for derivation details)

$$\frac{d\rho}{dt} = -i[H, \rho] + \sum_m (2L_m \rho L_m^\dagger - \{L_m^\dagger L_m, \rho\}), \quad (1)$$

with the Hamiltonian

$$H = H_S + \sum_{\alpha=L,R} (H_\alpha + H_{\alpha S}). \quad (2)$$

Here,  $H_S = \sum_{ij} (\mathbf{h}_S)_{ij} c_i^\dagger c_j$  is the Hamiltonian of the central system, where  $c_j$  is the annihilation operator at site  $j$  and  $(\mathbf{h}_S)_{ij}$  is the  $i$ -th row and  $j$ -th column element of the matrix  $\mathbf{h}_S$ , representing the hopping amplitude between sites  $i$  and  $j$ . The subscripts  $\alpha = L$  and  $\alpha = R$  denote the left and right leads, respectively, with the corresponding Hamiltonian  $H_\alpha = \sum_k \epsilon_{\alpha,k} d_{\alpha,k}^\dagger d_{\alpha,k}$ , where  $\epsilon_{\alpha,k}$  is the energy of the  $k$ -th mode of the  $\alpha$ -lead and  $d_{\alpha,k}^\dagger$  ( $d_{\alpha,k}$ ) creates (annihilates) a particle in this mode. The term  $H_{\alpha S} = \sum_{jk} t_{\alpha,kj} d_{\alpha,k}^\dagger c_j + h.c.$  describes the coupling between the  $\alpha$ -lead and the system, where  $t_{\alpha,kj}$  is the tunneling strength. The Lindblad operators  $L_m$  in Eq. (1) describe particle gain or loss in the central system. Their

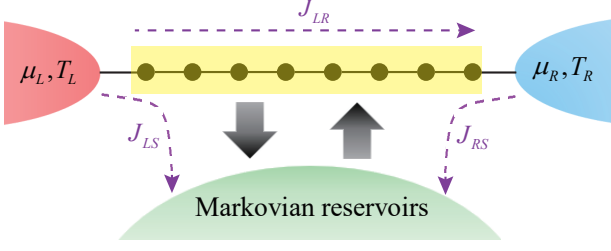


Figure 1: Model scheme: A central system (yellow region) is coupled to two leads (left and right) with temperatures  $T_{L(R)}$  and chemical potentials  $\mu_{L(R)}$ . It also connects to Markovian reservoirs (green region) for particle transfer. The current splits into three components (Eq. (8)):  $J_{LR}$ ,  $J_{LS}$ , and  $J_{RS}$ .  $J_{LR}$  is described by the Landauer-Büttiker formula, while the others arise from particle exchange with the reservoirs.

form and strength depend on the system-reservoir coupling and reservoir correlation functions [108], and can generally be written as

$$L_{1,i} = \sum_j u_{ij} c_j \quad \text{and} \quad L_{2,i} = \sum_j v_{ij} c_j^\dagger, \quad (3)$$

where  $L_{1,i}$  and  $L_{2,i}$  represent the loss and gain channels, respectively, which can be either on-site or non-local.

*Generic formula.*— We now derive the particle and energy currents for the above system, denoted as  $J^0$  and  $J^1$ , respectively. The particle (energy) currents flowing out of the left lead and into the right lead are, respectively,  $J_L^0 = -\frac{dN_L}{dt}$  ( $J_L^1 = -\frac{d\langle H_L \rangle}{dt}$ ) and  $J_R^0 = \frac{dN_R}{dt}$  ( $J_R^1 = \frac{d\langle H_R \rangle}{dt}$ ) [108], where  $N_\alpha = \sum_k d_{\alpha,k}^\dagger d_{\alpha,k}$  and  $\langle H_\alpha \rangle$  are the particle number and energy of the  $\alpha$ -lead, respectively. Using  $J_L^0 = -\frac{i}{\hbar} [H, N_L]$  and  $J_L^1 = -\frac{i}{\hbar} [H, H_L]$ , we can compute the currents flowing out of the left lead:

$$J_L^0 = \frac{1}{\hbar} \sum_k (t_{L,kj} G_{SL,jk}^< - t_{L,kj}^* G_{LS,kj}^<), \quad (4)$$

$$J_L^1 = \frac{1}{\hbar} \sum_k \epsilon_{L,k} (t_{L,kj} G_{SL,jk}^< - t_{L,kj}^* G_{LS,kj}^<).$$

To trace out the leads, we use the Lindblad-Keldysh formalism [109–112]. The system's partition function can be written as  $Z = \text{tr} \rho(t) = \int D[\bar{\psi}, \psi] e^{i\mathcal{S}[\bar{\psi}, \psi]}$  [108], where  $\mathcal{S}$  is the Keldysh action and  $\psi = (\psi^+, \psi^-)$  are Grassmann variables defined on the upper and lower branches of the Keldysh contour. This description contains redundancy [109], and for computational convenience, a Keldysh rotation is often performed:  $\psi^1 = \frac{1}{\sqrt{2}}(\psi^+ + \psi^-)$ ,  $\psi^2 = \frac{1}{\sqrt{2}}(\psi^+ - \psi^-)$ ,  $\bar{\psi}^1 = \frac{1}{\sqrt{2}}(\bar{\psi}^+ - \bar{\psi}^-)$ , and  $\bar{\psi}^2 = \frac{1}{\sqrt{2}}(\bar{\psi}^+ + \bar{\psi}^-)$ . In this basis, the Keldysh action  $\mathcal{S}$  of the central region can be rewritten as [108]

$$\mathcal{S} = \int dt (\bar{\psi}^1 \quad \bar{\psi}^2) \begin{pmatrix} i\partial_t - \mathbf{X} & i\mathbf{Y} \\ 0 & i\partial_t - \mathbf{X}^\dagger \end{pmatrix} \begin{pmatrix} \psi^1 \\ \psi^2 \end{pmatrix}, \quad (5)$$

where  $\mathbf{X} = \mathbf{h}_S - i\mathbf{P} - i\mathbf{Q}$  describes the damping dynamics [113, 114], and  $\mathbf{Y} = 2(\mathbf{P} - \mathbf{Q})$  describes the imbalance between loss and gain. Note that the quantities in bold-face are matrices. The elements of the matrices  $\mathbf{P}$  and  $\mathbf{Q}$  are  $P_{jk} = \sum_m u_{mj}^* u_{mk}$  and  $Q_{jk} = \sum_m v_{mj} v_{mk}^*$ , corresponding to the loss and gain terms, respectively. The system's retarded, advanced and Keldysh Green's functions are obtained by inverting the matrix (5):  $\mathbf{g}_S^R = \frac{1}{\omega - \mathbf{X}}$ ,  $\mathbf{g}_S^A = \frac{1}{\omega - \mathbf{X}^\dagger}$ ,  $\mathbf{g}_S^K = -\frac{1}{\omega - \mathbf{X}} i\mathbf{Y} \frac{1}{\omega - \mathbf{X}^\dagger}$ . Further combining the Langreth theorem [112, 115], after introducing the leads, one can obtain [108]:

$$\mathbf{G}_S^> = i\mathbf{G}_S^R (f_L \Gamma_L + f_R \Gamma_R - \Gamma_L - \Gamma_R - 2\mathbf{P}) \mathbf{G}_S^A, \quad (6)$$

$$\mathbf{G}_S^< = i\mathbf{G}_S^R (f_L \Gamma_L + f_R \Gamma_R + 2\mathbf{Q}) \mathbf{G}_S^A,$$

where  $f_\alpha = \frac{1}{e^{(\omega - \mu_\alpha)/k_B T_\alpha} + 1}$  is the Fermi distribution associated to the  $\alpha$ -lead,  $\mathbf{G}_S^R = (\mathbf{G}_S^A)^\dagger = [(\mathbf{g}_S^R)^{-1} - \tilde{\Sigma}_L^R - \tilde{\Sigma}_R^R]^{-1}$ , and  $\Gamma_\alpha = i(\tilde{\Sigma}_\alpha^R - \tilde{\Sigma}_\alpha^A)$  is the spectral density, with the lead self-energy being given by  $\tilde{\Sigma}_\alpha^R = \Sigma_{S\alpha}^R \mathbf{g}_\alpha^R \Sigma_{\alpha S}^R$  ( $\alpha \in \{L, R\}$ ). The Langreth theorem also provides the relationship between the full Green's function ( $\mathbf{G}$ ) and the bare Green's function ( $\mathbf{g}$ ):

$$\mathbf{G}_{LS}^< = \mathbf{g}_{LS}^< \Sigma_{LS}^A \mathbf{G}_S^A + \mathbf{g}_{LS}^R \Sigma_{LS}^R \mathbf{G}_S^< + \mathbf{g}_{LS}^< \Sigma_L^< \mathbf{G}_{LS}^A, \quad (7)$$

$$\mathbf{G}_{SL}^< = \mathbf{G}_S^< \Sigma_{SL}^A \mathbf{g}_L^A + \mathbf{G}_S^R \Sigma_{SL}^R \mathbf{g}_L^< + \mathbf{G}_{SL}^R \Sigma_L^< \mathbf{g}_L^A.$$

By substituting Eq. (7) into Eq. (4), the Green's functions of the system-lead coupling,  $\mathbf{G}_{LS}$  and  $\mathbf{G}_{SL}$ , can be replaced by the system Green's function,  $\mathbf{G}_S$ . Further applying Eq. (6), the current flowing out of the left lead,  $J_L^\lambda$ , can be derived (see Supplemental Material [108] for details), where  $\lambda = 0$  and  $\lambda = 1$  correspond to particle and energy currents, respectively. A similar procedure gives the current flowing into the right lead,  $J_R^\lambda$ . Due to the exchange of particles and energy between the central system and the environment, the currents flowing out of the left lead and into the right lead may differ, i.e.,  $J_L^\lambda \neq J_R^\lambda$  in the steady state. The total current through the system is given by  $J^\lambda = \frac{1}{2}(J_L^\lambda + J_R^\lambda)$ . These currents can be divided into three parts (see Fig. 1):

$$J^\lambda = J_{LR}^\lambda + J_{LS}^\lambda - J_{RS}^\lambda, \quad (8)$$

$$J_{LR}^\lambda = \int \frac{d\omega}{2\hbar} (f_L - f_R) \omega^\lambda \text{Tr}[\Gamma_L \mathbf{G}_S^R \Gamma_R \mathbf{G}_S^A + \Gamma_R \mathbf{G}_S^R \Gamma_L \mathbf{G}_S^A],$$

$$J_{L(R)S}^\lambda = \int \frac{d\omega}{\hbar} f_{L(R)} \omega^\lambda \text{Tr}[\Gamma_{L(R)} \mathbf{G}_S^R \mathbf{P} \mathbf{G}_S^A]$$

$$+ \int \frac{d\omega}{\hbar} (f_{L(R)} - 1) \omega^\lambda \text{Tr}[\Gamma_{L(R)} \mathbf{G}_S^R \mathbf{Q} \mathbf{G}_S^A].$$

The terms  $J_{LR}^\lambda$ , representing the Landauer-Büttiker formula, and  $J_{LS}^\lambda - J_{RS}^\lambda$  describe the current between two leads through the central system and through the reservoirs, respectively. Here,  $J_{L(R)S}$  consists of two parts: one describes the current from the leads to the loss channel through the central system, proportional to the particle distribution  $f_{L(R)}$ , and the other describes the current

from the gain channel to the leads through the central system, proportional to the hole distribution  $1 - f_{L(R)}$ .

*Applications.*— We will now discuss the interesting physical phenomena presented in Eq. (8). For convenience, the models we will discuss below as examples include only the nearest-neighbor hopping, i.e.,  $(\mathbf{h}_S)_{ij} = -t_S \delta_{i,j\pm 1}$ , where  $t_S$  is the hopping strength, and unless otherwise specified, we set  $t_S = 1$ .

To directly observe the effects of gain and loss on the current from Eq. (8), we assume  $f_L = f_R = f$ , meaning no chemical potential ( $\mu_L = \mu_R = \mu$ ) or temperature ( $T_L = T_R = T$ ) difference between the two leads, which results in no Landauer current  $J_{LR}^\lambda$ . From Eq. (8), we see that gain and loss can generate a current, except in two special cases, where the current vanishes. The first case occurs when the particle-to-hole ratio in the leads,  $n_p/n_h = f/(1-f)$ , matches the gain-to-loss ratio in the system,  $\mathbf{Q}/\mathbf{P}$ , such that the particle flow from the leads is exactly balanced by the gain and loss processes, leading to  $J_{LS}^\lambda = J_{RS}^\lambda = 0$  according to Eq. (8). In the high-temperature limit  $k_B T \gg t_S$ , the vanishing current condition simplifies to  $\ln \frac{\mathbf{Q}}{\mathbf{P}} = \ln \frac{f}{1-f} = \frac{\mu}{k_B T}$ . Fig. 2 (a) illustrates how the particle current  $J^0$  changes with  $\mu/k_B T$  and  $\gamma_g/\gamma_l$ , where the gain and loss terms are assumed to be onsite and uniform, namely  $L_{1,i} = \sqrt{\gamma_l} c_i$  and  $L_{2,i} = \sqrt{\gamma_g} c_i^\dagger$ . We observe that along the curve  $\ln(\gamma_g/\gamma_l) = \mu/k_B T$ ,  $J^0$  is zero, while on either side of this curve,  $J^0$  is nonzero and opposite in direction.

The second case, in which the added gain and loss terms do not generate a current, is when the system and the gain and loss terms have inversion symmetry (IS), i.e.,  $\mathcal{P}^{-1} O_{ij} \mathcal{P} = O_{N-i+1, N-j+1}$ , where the operator  $\mathbf{O}$  represents the Hamiltonian  $\mathbf{H}$ , the loss matrix  $\mathbf{P}$ , and the gain matrix  $\mathbf{Q}$  [116], and additionally, the spectral density matrix should satisfy  $\mathcal{P}^{-1} \mathbf{\Gamma}_L \mathcal{P} = \mathbf{\Gamma}_R$ . It is easy to show from Eq. (8) that in this case,  $J_{LS}^\lambda = J_{RS}^\lambda$ . In Fig. 2 (b1), we show an example of two sites with a local monitoring described by  $L_{1,j} = \sqrt{\gamma_j} c_j$ . In the limit  $\gamma_j \ll \omega$ , the current can be written analytically as [108]

$$J^0 \approx (\gamma_1 - \gamma_2) \Gamma \int \frac{d\omega}{h} f(\omega) \frac{|\omega + \frac{i\Gamma}{2}|^2 - 1}{|(\omega + \frac{i\Gamma}{2})^2 - 1|^2}, \quad (9)$$

where  $\Gamma = (\mathbf{\Gamma}_L)_{11} = (\mathbf{\Gamma}_R)_{NN}$ . When  $\gamma_1 = \gamma_2 = \gamma_0$ , i.e., both the system and the loss term preserve IS, the current  $J^0$  remains zero regardless of  $\gamma_0$ , as shown by the green line in Fig. 2 (b2). Breaking IS by removing the loss on one site ( $\gamma_1 \neq \gamma_2$ ) induces a current proportional to  $\gamma_1 - \gamma_2$ , as indicated by the red and blue lines in Fig. 2(b2). Thus, when an inversion-symmetric system couples to an environment, even weak particle gain or loss can generate a current if it breaks IS. This property can be used to measure the characteristics of the environment.

On the other hand, if the gain and loss terms preserve IS but the system does not, a current can also arise. We consider uniform onsite loss to preserve IS in the dissipa-

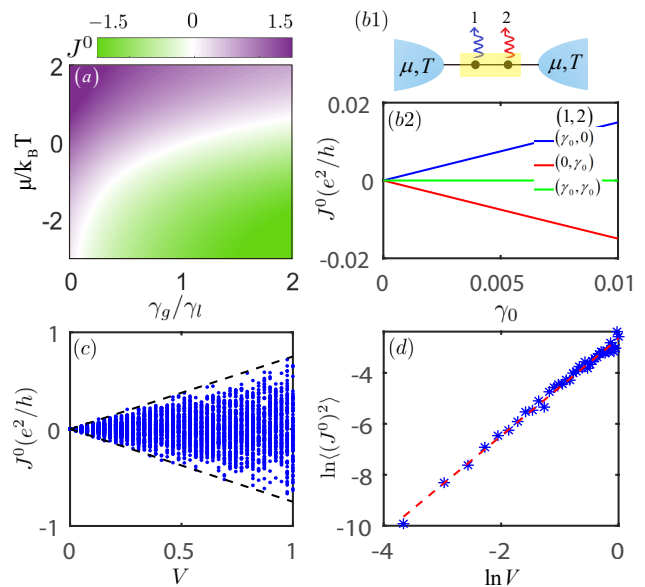


Figure 2: (a)  $J^0$  as a function of  $\gamma_g/\gamma_l$  and  $\mu/k_B T$ , in units of  $e^2/h$ , with  $k_B T = 20$ ,  $\gamma_l = 0.2$ , and the system size  $N = 40$ . (b1) Scheme of a two-site system with local monitoring. (b2)  $J^0$  as a function of monitoring strength  $\gamma_0$ . The blue and red curves represent monitoring at the first and second sites, respectively, while the green curve represents monitoring at both sites. (c)  $J^0$  as a function of disorder strength  $V$  with 200 samples and  $N = 100$ . The black dashed line represents the envelope curve of the current. (d) The sample average of  $\langle (J^0)^2 \rangle$ . The red dashed line is the fitting function  $\langle (J^0)^2 \rangle \sim V^{1.91}$ . Other parameters are (b-d)  $\mu = 0.1$ ,  $k_B T = 10^{-4}$ ,  $\gamma_l = 0.1$ , and (a-d)  $t_S = 1$ ,  $(\mathbf{\Gamma}_L)_{11} = (\mathbf{\Gamma}_R)_{NN} = 1.1$ .

tion term, and introduce a disorder potential  $\sum_j V_j c_j^\dagger c_j$  to break IS in the system Hamiltonian  $H_S$ , with  $V_j$  randomly distributed in  $[-V, V]$ . In one dimension, all eigenstates are localized even for arbitrarily weak disorder. As shown in Fig. 2(c), the current  $J^0$  remains zero at  $V = 0$  due to IS, but grows with increasing  $V$ , exhibiting strong sample-to-sample fluctuations. These behaviors can be analytically understood using a two-site model (see Supplemental Materials [108]): in the weak disorder limit,  $J^0 \approx \frac{c}{2}(V_1 - V_2)$  [108], where  $c$  depends on the loss strength  $\gamma$  and the Fermi distribution.  $J^0$  thus vanishes for symmetric potentials  $V_1 = V_2$ , and reaches  $\pm cV$  for maximal asymmetry  $V_1 = -V_2 = \pm V$ , forming linear envelope bounds. In the strong disorder regime, resonant tunneling dominates, and the envelope of  $J^0$  fluctuations saturates to a  $V$ -independent value [108]. This crossover reflects competition between dissipation and disorder. Fig. 2(d) shows that the sample average of  $\langle (J^0)^2 \rangle$  scales with disorder strength as  $\langle (J^0)^2 \rangle \sim V^2$ . In contrast to closed systems, where disorder suppresses transport, here it can induce current. With spin-dependent disorder, one can further generate spin-polarized currents or even pure spin currents without net charge flow [108].

We then consider the current when there is a chemical

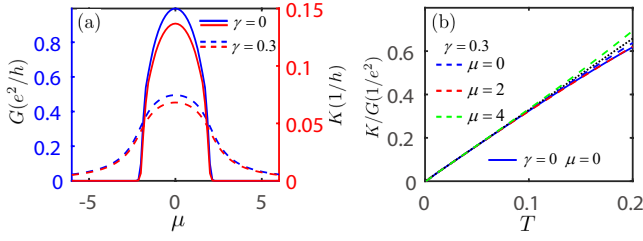


Figure 3: (a)  $G$  and  $K$  as functions of the chemical potential  $\mu$  with temperature  $T = 0.04$ . (b) The ratio  $K/G$  as a function of  $T$ .  $\mu = 0$ ,  $\mu = 2$ , and  $\mu = 4$  are located inside the band, at the band edge, and outside the band, respectively. The black dotted line represents the Wiedemann-Franz law. Here we take  $k_B = 1$ ,  $t_S = 1$  and  $N = 80$ .

potential and temperature gradient between the leads, i.e.,  $f_L \neq f_R$ . We set  $\mu_R = \mu$ ,  $T_R = T$ ,  $f_R = f$ , and  $\mu_L = \mu + \delta\mu$ ,  $T_L = T + \delta T$ ,  $f_L = f + \delta f$ . For convenience, we rewrite the current in Eq. (8) as two parts:

$$J^\lambda = J_0^\lambda + \delta J_1^\lambda, \quad (10)$$

where  $J_0^\lambda$  denotes the net current under equilibrium conditions ( $\delta f = 0$ ), and  $\delta J_1^\lambda$ , referred to as the response current, describes the current induced when  $\delta f \neq 0$ . From Eq. (8), it is easy to obtain

$$\delta J_1^\lambda = \int \frac{d\omega}{h} \omega^\lambda \delta f(\omega) \tau_1(\omega), \quad (11)$$

where  $\tau_1 = \tau_{11} + \tau_{12}$ , with  $\tau_{11} = \frac{1}{2} \text{Tr}[\mathbf{\Gamma}_L \mathbf{G}_S^R \mathbf{\Gamma}_R \mathbf{G}_S^A + \mathbf{\Gamma}_R \mathbf{G}_S^R \mathbf{\Gamma}_L \mathbf{G}_S^A]$  describing direct transmission between the leads and  $\tau_{12} = \text{Tr}[\mathbf{\Gamma}_L \mathbf{G}_S^R (\mathbf{P} + \mathbf{Q}) \mathbf{G}_S^A]$  accounting for indirect transmission via the reservoirs. For inversion-symmetric systems,  $J_0 = 0$  and the current  $J = \delta J_1$  follows thermodynamic gradients (from high to low  $\mu$  and  $T$ ). When IS is broken,  $J_0$  and  $\delta J_1$  compete, adding constructively when aligned or being dominated by the larger term when opposed.

The electrical conductance  $G$ , determined by the response current  $\delta J_1^0$ , depends on the transmission function  $\tau_1$  via  $G = \frac{e^2}{h} \int d\omega \frac{\delta f(\omega)}{\delta \mu} \tau_1(\omega)$  [108]. The size dependence of  $G$  is encoded in  $\tau_1$ : without gain and loss ( $\tau_{12} = 0$ ), transport is ballistic and  $\tau_{11}$  is size-independent; with gain or loss,  $\tau_{11}$  decays exponentially due to particles scattering into reservoirs, while  $\tau_{12}$ , which arises from reservoir channels whose number increases with system size, remains nearly size-independent [108]. Thus, in the thermodynamic limit, the conductance is dominated by indirect transmission [117].

The transmission function  $\tau_1$  also determines the thermal conductance  $K$  [79, 108, 118]. In the low-temperature limit, the ratio  $K/G$  follows the Wiedemann-Franz law  $K/G \approx \mathcal{L}T$ , with  $\mathcal{L} = \frac{\pi^2}{3} (\frac{k_B}{e})^2$  being the Lorenz number. Without dissipation, both  $G$  and  $K$  are finite only within the energy band [Fig. 3(a)],

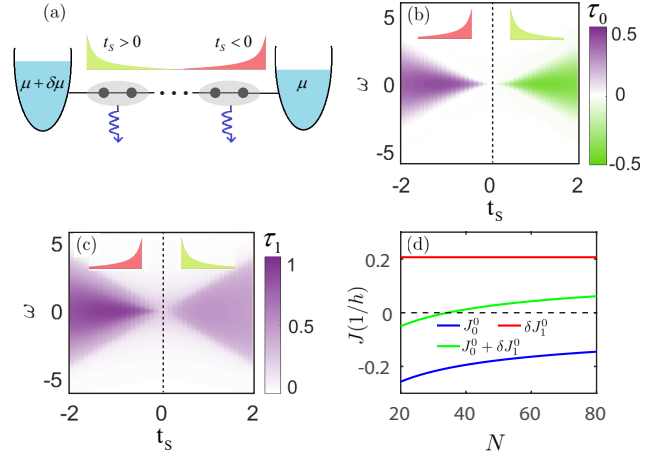


Figure 4: (a) Schematic of the setup to study transport in a system with NHSE caused by bond loss. The transmission functions (b)  $\tau_0$  and (c)  $\tau_1$  as a function of  $t_S$  and  $\omega$  for a system with size  $N = 80$ . (d) The variation of  $J_0^0$ ,  $\delta J_1^0$ , and  $J^0 = J_0^0 + \delta J_1^0$  with system size, with  $t_S = 3$  fixed. Other parameters: (b-d)  $\gamma_- = 1$ ,  $\mu = 0.12$ ; (c-d)  $\delta\mu = 0.6$ .

and the law holds only there [Fig. 3(b)] [119]. We then consider the case where each site is subject to equal loss and gain ( $\gamma_l = \gamma_g = \gamma$ ), which causes the conductances to broaden and smooth out near the band edge [Fig. 3(a)], allowing the Wiedemann-Franz law to hold both inside and outside the band [Fig. 3(b)].

Eq. (8) also applies to non-on-site gain or loss. As an example, we consider the bond-loss  $L_j = \sqrt{\gamma_-} (c_j - ic_{j+1})$ , which induces the non-Hermitian skin effect (NHSE) in this system: all eigenstates localize at the left (right) end for  $t_S > 0$  ( $t_S < 0$ ) [120, 121] [Fig. 4(a)]. In the zero-temperature limit, the current is  $J_0^0 = \int_{-\infty}^{\mu} \frac{d\omega}{h} \tau_0(\omega)$  and  $\delta J_1^0 = \int_{\mu}^{\mu + \delta\mu} \frac{d\omega}{h} \tau_1(\omega)$ , where  $\tau_0$  and  $\tau_1$  are the transmission functions [108]. Figures 4(b) and (c) show  $\tau_0$  and  $\tau_1$  as functions of frequency  $\omega$  and  $t_S$ , respectively. It can be seen that  $\tau_0$  is positive (negative) when skin modes localize on the right (left) end, so  $J_0^0$  flows in the same direction as the skin modes when  $\mu_L = \mu_R$ . Under a voltage bias ( $\delta\mu \neq 0$ ), the response current  $\delta J_1^0$  always flows from high to low  $\mu$ , as shown in Fig. 4(c). Thus, if the bias opposes the skin direction, the direction of the total current depends on the competition between  $J_0^0$  and  $\delta J_1^0$ . In the thermodynamic limit,  $J_0^0$  decreases with increasing system size and, for  $|t_S| \geq |\gamma_-|$ , satisfies:  $J_0^0 \sim N^{-0.5}$  for  $\mu \geq 0$  and  $J_0^0 \sim \frac{e^{-N}}{N}$  for  $\mu < 0$  [108]. This implies that the current corresponding to the NHSE vanishes as the system size tends to infinity, while  $\delta J_1^0$  does not depend on the system size [Fig. 4(d)]. Therefore, the direction of the current  $J^0$  can be changed by altering the system size to change  $J_0^0$  or by changing  $\delta\mu$  to adjust  $\delta J_1^0$ .

*Discussion and conclusion.*— We have derived a general formula for the current through a region with particle

exchange with the environment, and further demonstrate its usefulness by identifying several novel transport features: (I) A current is generated when gain or loss terms lack inversion symmetry; (II) Disorder can induce current; (III) Gain and loss make the thermal and electrical conductances continuous and cause their ratio to satisfy the Wiedemann-Franz law inside and outside the energy band; (IV) The bond loss-induced NHSE and the current caused by the chemical potential difference exhibit an interesting competition. Our work establishes a versatile framework for studying the influence of particle gain or loss on transport phenomena, opening avenues for future studies of open and non-Hermitian physics.

This work is supported by National Key R&D Program of China under Grant No.2022YFA1405800, the Key-Area Research and Development Program of Guangdong Province (Grant No.2018B030326001), Guangdong Provincial Key Laboratory(Grant No.2019B121203002).

---

\* Corresponding author: wangyc3@sustech.edu.cn

- [1] S. Datta, *Electronic Transport in Mesoscopic Systems*, (Cambridge University Press, 1997).
- [2] Y. Nazarov and Y. Blanter, *Quantum Transport: Introduction to Nanoscience*, (Cambridge University Press, 2009).
- [3] G. T. Landi, D. Poletti, and G. Schaller, Nonequilibrium boundary-driven quantum systems: Models, methods, and properties, *Rev. Mod. Phys.* **94**, 045006 (2022).
- [4] B. Bertini, F. Heidrich-Meisner, C. Karrasch, T. Prosen, R. Steinigeweg, and M. Žnidarič, Finite-temperature transport in one-dimensional quantum lattice models, *Rev. Mod. Phys.* **93**, 025003 (2021).
- [5] Y. Dubi and M. Di Ventra, Colloquium: Heat flow and thermoelectricity in atomic and molecular junctions, *Rev. Mod. Phys.* **83**, 131 (2011).
- [6] F. Verstraete, M. M. Wolf, and J. Ignacio Cirac, Quantum computation and quantum-state engineering driven by dissipation, *Nat. Phys.* **5**, 633 (2009).
- [7] A. Dhar, Heat transport in low-dimensional systems, *Advances in Physics* **57**, 457 (2008).
- [8] R. Landauer, Electrical resistance of disordered one-dimensional lattices, *Philos. Mag.* **21**, 863 (1970).
- [9] M. Büttiker, Four-Terminal Phase-Coherent Conductance, *Phys. Rev. Lett.* **57**, 1761 (1986).
- [10] C.-C. Chien, S. Peotta, and M. D. Ventra, Quantum transport in ultracold atoms, *Nat. Phys.* **11**, 998 (2015).
- [11] C.-C. Chien, M. D. Ventra, and M. Zwolak, Landauer, Kubo, and microcanonical approaches to quantum transport and noise: A comparison and implications for cold-atom dynamics, *Phys. Rev. A* **90**, 023624 (2014).
- [12] J.-P. Brantut, J. Meineke, D. Stadler, S. Krinner, and T. Esslinger, Conduction of ultracold fermions through a mesoscopic channel, *Science* **337**, 1069 (2012).
- [13] J.-P. Brantut, C. Grenier, J. Meineke, D. Stadler, S. Krinner, C. Kollath, T. Esslinger, and A. Georges, A thermoelectric heat engine with ultracold atoms, *Science* **342**, 713 (2013).
- [14] S. Krinner, D. Stadler, D. Husmann, J.-P. Brantut, and T. Esslinger, Observation of quantized conductance in neutral matter, *Nature (London)* **517**, 64 (2015).
- [15] A. Kurnosov, L.J. Fernández-Alcázar, A. Ramos, B. Shapiro, and T. Kottos, Optical Kinetic Theory of Non-linear Multimode Photonic Networks, *Phys. Rev. Lett.* **132**, 193802 (2024).
- [16] M. Lian, Y. Geng, Y.-J. Chen, Y. Chen, and J.-T. Lü, Coupled Thermal and Power Transport of Optical Waveguide Arrays: Photonic Wiedemann-Franz Law and Rectification Effect, *Phys. Rev. Lett.* **133**, 116303 (2024).
- [17] T. Yamamoto and K. Watanabe, Nonequilibrium Green's Function Approach to Phonon Transport in Defective Carbon Nanotubes, *Phys. Rev. Lett.* **96**, 255503 (2006).
- [18] Y. Imry and R. Landauer, Conductance viewed as transmission, *Rev. Mod. Phys.* **71**, S306 (1999).
- [19] H. Ritsch, P. Domokos, F. Brennecke, and T. Esslinger, Cold atoms in cavity-generated dynamical optical potentials, *Rev. Mod. Phys.* **85**, 553 (2013).
- [20] D. Dreon, A. Baumgärtner, X. Li, S. Hertlein, T. Esslinger, and T. Donner, Self-oscillating pump in a topological dissipative atom-cavity system, *Nature* **608**, 494 (2022).
- [21] H. Weimer, M. Müller, I. Lesanovsky, P. Zoller, and H. P. Büchler, A Rydberg quantum simulator, *Nat. Phys.* **6**, 382 (2010).
- [22] M. Müller, S. Diehl, G. Pupillo, and P. Zoller, Engineered open systems and quantum simulations with atoms and ions, *Advances in Atomic, Molecular, and Optical Physics* **61**, 1 (2012).
- [23] H. Krauter, C. A. Muschik, K. Jensen, W. Wasilewski, J. M. Petersen, J. I. Cirac, and E. S. Polzik, Entanglement Generated by Dissipation and Steady State Entanglement of Two Macroscopic Objects, *Phys. Rev. Lett.* **107**, 080503 (2011).
- [24] D. Kienzler, H.-Y. Lo, B. Keitch, L. de Clercq, F. Leupold, F. Lindenefser, M. Marinelli, V. Negnevitsky, and J. P. Home, Quantum harmonic oscillator state synthesis by reservoir engineering, *Science* **347**, 53 (2015).
- [25] Z. Leghtas, S. Touzard, I. M. Pop, A. Kou, B. Vlastakis, A. Petrenko, K. M. Sliwa, A. Narla, S. Shankar, M. J. Hatridge, M. Reagor, L. Frunzio, R. J. Schoelkopf, M. Mirrahimi, and M. H. Devoret, Confining the state of light to a quantum manifold by engineered two-photon loss, *Science* **347**, 853 (2015).
- [26] P. M. Harrington, E. J. Mueller, and K. W. Murch, Engineered dissipation for quantum information science, *Nat. Rev. Phys.* **4**, 660 (2022).
- [27] S. Viciani, M. Lima, M. Bellini, and F. Caruso, Observation of Noise-Assisted Transport in an All-Optical Cavity-Based Network, *Phys. Rev. Lett.* **115**, 083601 (2015).
- [28] C. Maier, T. Brydges, P. Jurcevic, N. Trautmann, C. Hempel, B. P. Lanyon, P. Hauke, R. Blatt, and C. F. Roos, Environment-Assisted Quantum Transport in a 10-Qubit Network, *Phys. Rev. Lett.* **122**, 050501 (2019).
- [29] T. Tomita, S. Nakajima, I. Danshita, Y. Takasu, and Y. Takahashi, Observation of the Mott insulator to superfluid crossover of a driven-dissipative Bose-Hubbard system, *Science Advances* **3**, e1701513 (2017).
- [30] N. Dogra, M. Landini, K. Kroeger, L. Hruby, T. Donner, and T. Esslinger, Dissipation-induced structural instability and chiral dynamics in a quantum gas, *Science* **366**, 1496 (2019).
- [31] R. Bouganne, M. Bosch Aguilera, A. Ghermaoui, J.

- Beugnon, and F. Gerbier, Anomalous decay of coherence in a dissipative many-body system, *Nat. Phys.* **16**, 21 (2020).
- [32] J. Barreiro, M. Müller, P. Schindler, D. Nigg, T. Monz, M. Chwalla, M. Hennrich, C. Roos, P. Zoller, and R. Blatt, An open-system quantum simulator with trapped ions, *Nature* **470**, 486 (2011).
- [33] N. Syassen, D. M. Bauer, M. Lettner, T. Volz, D. Dietze, J. J. Garcia-Ripoll, J. I. Cirac, G. Rempe, and S. Dürr, Strong dissipation inhibits losses and induces correlations in cold molecular gases, *Science* **320**, 1329 (2008).
- [34] V. A. Brazhnyi, V. V. Konotop, V. M. Pérez-García, and H. Ott, Dissipation-induced coherent structures in Bose-Einstein condensates, *Phys. Rev. Lett.* **102**, 144101 (2009).
- [35] J. Li, A. K. Harter, J. Liu, L. de Melo, Y. N. Joglekar, and L. Luo, Observation of parity-time symmetry breaking transitions in a dissipative Floquet system of ultracold atoms, *Nat. Commun.* **10**, 855 (2019).
- [36] A. Blais, A. L. Grimsmo, S. M. Girvin, and A. Wallraff, Circuit quantum electrodynamics, *Rev. Mod. Phys.* **93**, 025005 (2021).
- [37] M. Fitzpatrick, N. M. Sundaresan, A. C. Y. Li, J. Koch, and A. A. Houck, Observation of a Dissipative Phase Transition in a One-Dimensional Circuit QED Lattice, *Phys. Rev. X* **7**, 011016 (2017).
- [38] R. Labouvie, B. Santra, S. Heun, and H. Ott, Bistability in a driven-dissipative superfluid, *Phys. Rev. Lett.* **116**, 235302 (2016).
- [39] L. Corman, P. Fabritius, S. Häusler, J. Mohan, L. H. Dogra, D. Husmann, M. Lebrat, and T. Esslinger, Quantized conductance through a dissipative atomic point contact, *Phys. Rev. A* **100**, 053605 (2019).
- [40] M. Lebrat, S. Häusler, P. Fabritius, D. Husmann, L. Corman, and T. Esslinger, Quantized conductance through a spin-selective atomic point contact, *Phys. Rev. Lett.* **123**, 193605 (2019).
- [41] M.-Z. Huang, J. Mohan, A.-M. Visuri, P. Fabritius, M. Talebi, S. Wili, S. Uchino, T. Giamarchi, and T. Esslinger, Superfluid signatures in a dissipative quantum point contact, *Phys. Rev. Lett.* **130**, 200404 (2023).
- [42] R. El-Ganainy, K.G. Makris, M. Khajavikhan, Z.H. Musslimani, S. Rotter, and D.N. Christodoulides, Non-Hermitian physics and PT symmetry, *Nat. Phys.* **14**, 11 (2018).
- [43] Ş. K. Özdemir, S. Rotter, F. Nori, and L. Yang, Parity-time symmetry and exceptional points in photonics, *Nat. Mater.* **18**, 783 (2019).
- [44] Y. Sun, T. Shi, Z. Liu, Z. Zhang, L. Xiao, S. Jia, and Y. Hu, Fractional Quantum Zeno Effect Emerging from Non-Hermitian Physics, *Phys. Rev. X* **13**, 031009 (2023).
- [45] L. Xiao, T. Deng, K. Wang, Z. Wang, W. Yi, and P. Xue, Observation of Non-Bloch Parity-Time Symmetry and Exceptional Points, *Phys. Rev. Lett.* **126**, 230402 (2021); P. Xue, Q. Lin, K. Wang, L. Xiao, S. Longhi, and W. Yi, Self acceleration from spectral geometry in dissipative quantum-walk dynamics, *Nat. Commun.* **15**, 4381 (2024); L. Xiao, W.-T. Xue, F. Song, Y.-M. Hu, W. Yi, Z. Wang, and P. Xue, Observation of Non-Hermitian Edge Burst in Quantum Dynamics, *Phys. Rev. Lett.* **133**, 070801 (2024).
- [46] J. Zhu, Y.-L. Mao, H. Chen, K.-X. Yang, L. Li, B. Yang, Z.-D. Li, and J. Fan, Observation of Non-Hermitian Edge Burst Effect in One-Dimensional Photonic Quantum Walk, *Phys. Rev. Lett.* **132**, 203801 (2024).
- [47] E. Zhao, Z. Wang, C. He, T. F. J. Poon, K. K. Pak, Y.-J. Liu, P. Ren, X.-J. Liu, and G.-B. Jo, Two-dimensional non-Hermitian skin effect in an ultracold Fermi gas, *Nature* **637**, 565 (2025).
- [48] V. Maurya, H. Zhang, D. Kowsari, A. Kuo, D. M. Hartsell, C. Miyamoto, J. Liu, S. Shanto, E. Vlachos, A. Zarassi, K. W. Murch, and E. M. Levenson-Falk, On-Demand Driven Dissipation for Cavity Reset and Cooling, *PRX Quantum* **5**, 020321 (2024).
- [49] H. Hodaei, M.-A. Miri, M. Heinrich, D. N. Christodoulides, and M. Khajavikhan, Parity-time-symmetric microring lasers, *Science* **346**, 975 (2014).
- [50] L. A. Coldren, S. W. Corzine, M. L. Mašanović, *Diode Lasers and Photonic Integrated Circuits*, Wiley, 2012.
- [51] S. Diehl, A. Micheli, A. Kantian, B. Kraus, H. P. Büchler, and P. Zoller, Quantum states and phases in driven open quantum systems with cold atoms, *Nat. Phys.* **4**, 878 (2008); S. Diehl, A. Tomadin, A. Micheli, R. Fazio, and P. Zoller, Dynamical phase transitions and instabilities in open atomic many-body systems, *Phys. Rev. Lett.* **105**, 015702 (2010); S. Diehl, E. Rico, M. A. Baranov, and P. Zoller, Topology by dissipation in atomic quantum wires, *Nat. Phys.* **7**, 971 (2011).
- [52] F. Carollo, A. Lasanta, and I. Lesanovsky, Exponentially Accelerated Approach to Stationarity in Markovian Open Quantum Systems through the Mpemba Effect, *Phys. Rev. Lett.* **127**, 060401 (2021); A. K. Chatterjee, S. Takada, and H. Hayakawa, Quantum Mpemba Effect in a Quantum Dot with Reservoirs, *Phys. Rev. Lett.* **131**, 080402 (2023).
- [53] H.-P. Breuer, E.-M. Laine, J. Piilo, and B. Vacchini, Colloquium: Non-Markovian dynamics in open quantum systems, *Rev. Mod. Phys.* **88**, 021002 (2016); I. de Vega and D. Alonso, Dynamics of non-Markovian open quantum systems, *Rev. Mod. Phys.* **89**, 015001 (2017).
- [54] E. J. Bergholtz, J. C. Budich, and F. K. Kunst, Exceptional topology of non-Hermitian systems, *Rev. Mod. Phys.* **93**, 015005 (2021).
- [55] H. Weimer, A. Kshetrimayum, and R. Orús, Simulation methods for open quantum many-body systems, *Rev. Mod. Phys.* **93**, 015008 (2021).
- [56] M. Esposito, U. Harbola, and S. Mukamel, Nonequilibrium fluctuations, fluctuation theorems, and counting statistics in quantum systems, *Rev. Mod. Phys.* **81**, 1665 (2009).
- [57] T. Prosen and I. Pižorn, Quantum phase transition in a far-from-equilibrium steady state of an XY spin chain, *Phys. Rev. Lett.* **101**, 105701 (2008).
- [58] H. T. Mebrahtu, I. V. Borzenets, H. Zheng, Y. V. Bomze, A. I. Smirnov, S. Florens, H. U. Baranger, and G. Finkelstein, Observation of Majorana quantum critical behaviour in a resonant level coupled to a dissipative environment, *Nat. Phys.* **9**, 732 (2013); H. T. Mebrahtu, I. V. Borzenets, D. E. Liu, H. Zheng, Y. V. Bomze, A. I. Smirnov, H. U. Baranger, and G. Finkelstein, Quantum phase transition in a resonant level coupled to interacting leads, *Nature (London)* **488**, 61 (2012).
- [59] M. V. Medvedyeva, M. T. Čubrović, and S. Kehrein, Dissipation-induced first-order decoherence phase transition in a noninteracting fermionic system, *Phys. Rev. B* **91**, 205416 (2015).
- [60] K. Shastri and F. Monticone, Dissipation-induced topological transitions in continuous Weyl materials, *Phys.*

- Rev. Res. **2**, 033065 (2020).
- [61] M. Soriente, T. L. Heugel, K. Arimitsu, R. Chitra, and O. Zilberberg, Distinctive class of dissipation-induced phase transitions and their universal characteristics, Phys. Rev. Res. **3**, 023100 (2021).
- [62] W. Nie, M. Antezza, Y.-X. Liu, and F. Nori, Dissipative topological phase transition with strong system-environment coupling, Phys. Rev. Lett. **127**, 250402 (2021).
- [63] K. Yamamoto, M. Nakagawa, N. Tsuji, M. Ueda, and N. Kawakami, Collective excitations and nonequilibrium phase transition in dissipative fermionic superfluids, Phys. Rev. Lett. **127**, 055301 (2021).
- [64] K. Kawabata, T. Numasawa, and S. Ryu, Entanglement Phase Transition Induced by the Non-Hermitian Skin Effect, Phys. Rev. X **13**, 021007 (2023).
- [65] E. I. R. Chiacchio, A. Nunnenkamp, and M. Brunelli, Nonreciprocal Dicke Model, Phys. Rev. Lett. **131**, 113602 (2023).
- [66] Y. Liu, Z. Wang, C. Yang, J. Jie, and Y. Wang, Dissipation-induced extended-localized transition, Phys. Rev. Lett. **132**, 216301 (2024).
- [67] L.-N. Wu, J. Nettersheim, J. Feß, A. Schnell, S. Burgardt, S. Hiebel, D. Adam, A. Eckardt, and A. Widera, Indication of critical scaling in time during the relaxation of an open quantum system, Nat. Commun. **15**, 1714 (2024).
- [68] S. Longhi, Dephasing-induced mobility edges in quasicrystals, Phys. Rev. Lett. **132**, 236301 (2024).
- [69] S. A. Gurvitz, Delocalization in the Anderson Model due to a Local Measurement, Phys. Rev. Lett. **85**, 812 (2000).
- [70] A. G. Yamilov, R. Sarma, B. Redding, B. Payne, H. Noh, and H. Cao, Position-Dependent Diffusion of Light in Disordered Waveguides, Phys. Rev. Lett. **112**, 023904 (2014).
- [71] M. Balasubrahmaniam, S. Mondal, and S. Mujumdar, Necklace-State-Mediated Anomalous Enhancement of Transport in Anderson-Localized non-Hermitian Hybrid Systems, Phys. Rev. Lett. **124**, 123901 (2020).
- [72] S. Weidemann, M. Kremer, S. Longhi, and A. Szameit, Coexistence of dynamical delocalization and spectral localization through stochastic dissipation, Nat. Photon. **15**, 576 (2021).
- [73] M. V. Medvedyeva, T. Prosen, and M. Žnidarič, Influence of dephasing on many-body localization, Phys. Rev. B **93**, 094205 (2016).
- [74] E. Zerah-Harush and Y. Dubi, Effects of disorder and interactions in environment assisted quantum transport, Phys. Rev. Res. **2**, 023294 (2020).
- [75] S. Longhi, Anderson Localization in Dissipative Lattices, Ann. Phys. **535**, 2200658 (2023).
- [76] A. Purkayastha, A. Dhar, and M. Kulkarni, Nonequilibrium phase diagram of a one-dimensional quasiperiodic system with a single-particle mobility edge, Phys. Rev. B **96**, 180204(R) (2017).
- [77] M. Saha, B. P. Venkatesh, and B. K. Agarwalla, Quantum transport in quasiperiodic lattice systems in the presence of Büttiker probes, Phys. Rev. B **105**, 224204 (2022).
- [78] A. M. Lacerda, J. Goold, and G. T. Landi, Dephasing enhanced transport in boundary-driven quasiperiodic chains, Phys. Rev. B **104**, 174203 (2021).
- [79] C. Chiaracane, A. Purkayastha, M. T. Mitchison, and J. Goold, Dephasing-enhanced performance in quasiperiodic thermal machines, Phys. Rev. B **105**, 134203 (2022);
- C. Chiaracane, M. T. Mitchison, A. Purkayastha, G. Haack, and J. Goold, Quasiperiodic quantum heat engines with a mobility edge, Phys. Rev. Res. **2**, 013093 (2020).
- [80] D. Dwiputra and F. P. Zen, Environment-assisted quantum transport and mobility edges, Phys. Rev. A **104**, 022205 (2021).
- [81] V. Balachandran, S. R. Clark, J. Goold, and D. Poletti, Energy current rectification and mobility edges, Phys. Rev. Lett. **123**, 020603 (2019).
- [82] Y. Imry, *Introduction to Mesoscopic Physics* (Oxford University Press, Oxford 2002).
- [83] W. Belzig, C. Bruder, and G. Schön, Local density of states in a dirty normal metal connected to a superconductor, Phys. Rev. B **54**, 9443 (1996); C. Li, S. Guéron, A. Chepelianskii, and H. Bouchiat, Full range of proximity effect probed with superconductor/graphene/superconductor junctions, Phys. Rev. B **94**, 115405 (2016).
- [84] F. Hellman, A. Hoffmann, Y. Tserkovnyak, G. S. D. Beach, E. E. Fullerton, C. Leighton, A. H. MacDonald, D. C. Ralph, D. A. Arena, H. A. Dürr, P. Fischer, J. Grollier, J. P. Heremans, T. Jungwirth, A. V. Kimel, B. Koopmans, I. N. Krivorotov, S. J. May, A. K. Petford-Long, J. M. Rondinelli, N. Samarth, I. K. Schuller, A. N. Slavin, M. D. Stiles, O. Tchernyshyov, A. Thiaville, and B. L. Zink, Interface-induced phenomena in magnetism, Rev. Mod. Phys. **89**, 025006 (2017).
- [85] Z. Wang, C. Tang, R. Sachs, Y. Barlas, and J. Shi, Proximity-Induced Ferromagnetism in Graphene Revealed by the Anomalous Hall Effect, Phys. Rev. Lett. **114**, 016603 (2015); J. B. S. Mendes, O. Alves Santos, L. M. Meireles, R. G. Lacerda, L. H. Vilela-Leão, F. L. A. Machado, R. L. Rodríguez-Suárez, A. Azevedo, and S. M. Rezende, Spin current to charge-current conversion and magnetoresistance in a hybrid structure of graphene and yttrium iron garnet, Phys. Rev. Lett. **115**, 226601 (2015).
- [86] C. W. J. Beenakker, Random-matrix theory of quantum transport, Rev. Mod. Phys. **69**, 731 (1997).
- [87] H. Schomerus, Quantum Noise and Self-Sustained Radiation of PT-Symmetric Systems, Phys. Rev. Lett. **104**, 233601 (2010).
- [88] O. Scarlatella, A. A. Clerk, R. Fazio, and M. Schiró, Dynamical Mean-Field Theory for Markovian Open Quantum Many-Body Systems, Phys. Rev. X **11**, 031018 (2021).
- [89] H. Fröml, A. Chiocchetta, C. Kollath, and S. Diehl, Fluctuation-Induced Quantum Zeno Effect, Phys. Rev. Lett. **122**, 040402 (2019).
- [90] M. Nakagawa, N. Tsuji, N. Kawakami, and M. Ueda, Dynamical Sign Reversal of Magnetic Correlations in Dissipative Hubbard Models, Phys. Rev. Lett. **124**, 147203 (2020).
- [91] T. Jin, M. Filippone, and T. Giamarchi, Generic transport formula for a system driven by Markovian reservoirs, Phys. Rev. B **102**, 205131 (2020).
- [92] D. Rossini, A. Ghermaoui, M.B. Aguilera, R. Vatré, R. Bouganne, J. Beugnon, F. Gerbier, and L. Mazza, Strong correlations in lossy one-dimensional quantum gases: From the quantum Zeno effect to the generalized Gibbs ensemble, Phys. Rev. A **103**, L060201 (2021).
- [93] T. Müller, M. Gievers, H. Fröml, S. Diehl, and A. Chiocchetta, Shape effects of localized losses in quantum wires:

- Dissipative resonances and nonequilibrium universality, *Phys. Rev. B* **104**, 15431 (2021).
- [94] V. Alba and F. Carollo, Noninteracting fermionic systems with localized losses: Exact results in the hydrodynamic limit, *Phys. Rev. B* **105**, 054303.
- [95] A.-M. Visuri, T. Giamarchi, and C. Kollath, Symmetry-Protected Transport through a Lattice with a Local Particle Loss, *Phys. Rev. Lett.* **129**, 056802 (2022); A.-M. Visuri, T. Giamarchi, and C. Kollath, Nonlinear transport in the presence of a local dissipation, *Phys. Rev. Res.* **5**, 013195 (2023).
- [96] A.-M. Visuri, J. Mohan, S. Uchino, M.-Z. Huang, T. Esslinger, and T. Giamarchi, DC transport in a dissipative superconducting quantum point contact, *Phys. Rev. Res.* **5**, 033095 (2023).
- [97] J. Ferreira, T. Jin, J. Mannhart, T. Giamarchi, and M. Filippone, *Phys. Rev. Lett.* **bf 132**, 136301 (2024).
- [98] A. R. Kolovsky, Effects of internal and external decoherence on the resonant transport and Anderson localization of fermionic particles in disordered tight-binding chains, *Phys. Rev. B* **110**, 035410 (2024).
- [99] G. Stefanucci, Kadanoff-Baym Equations for Interacting Systems with Dissipative Lindbladian Dynamics, *Phys. Rev. Lett.* **bf 133**, 066901 (2024).
- [100] K. Ganguly, M. Kulkarni, and B. K. Agarwalla, Transport in open quantum systems in presence of lossy channels, arXiv:2408.14399.
- [101] X. Cao, C. Jia, Y. Hu, and Z. Liang, Dissipative Nonlinear Thouless Pumping of Temporal Solitons, arXiv:2409.03450.
- [102] M.-Z. Huang, P. Fabritius, J. Mohan, M. Talebi, S. Wili, and T. Esslinger, Limited thermal and spin transport in a dissipative superfluid junction, arXiv:2412.08525.
- [103] G. Lindblad, On the generators of quantum dynamical semigroups, *Commun. Math. Phys.* **48**, 119 (1976).
- [104] H.-P. Breuer and F. Petruccione, *The Theory of Open Quantum Systems* (Oxford University Press, Oxford, 2002).
- [105] H. Carmichael, *An Open Systems Approach to Quantum Optics*, Lecture Notes in Physics Monographs Vol. 18 (Springer, Berlin, Heidelberg, 1993).
- [106] Á. Rivas, S. F. Huelga, and M. B. Plenio, Quantum non-Markovianity: characterization, quantification and detection, *Rep. Prog. Phys.* **77**, 094001 (2014); Á. Rivas, A. D. K. Plato, S. F. Huelga, and M. B. Plenio, Markovian master equations: a critical study, *New J. Phys.* **12**, 113032 (2010).
- [107] C. A. Brasil, F. F. Fanchini and R. J. Napolitano, A simple derivation of the Lindblad equation, *Rev. Bras. Ensino Fis.* **35**, 1 (2013).
- [108] See the Supplemental Material for details on: (I) the distinction between Markovian reservoirs and conventional leads; (II) the derivation of the Lindblad master equation; (III) the definitions of particle and energy currents; (IV) the Keldysh theory for open fermionic systems; (V) the derivation of the extended Landauer-Büttiker formula; (VI) the impact of inversion symmetry in gain/loss terms on current; (VII) current generation induced by disorder; (VIII) the response current and the Wiedemann-Franz law; and (IX) the variation of  $J_0^0$  with system size in the presence of the skin effect. The Supplemental Materials includes the references [2, 79, 109, 118, 122–127].
- [109] L. M. Sieberer, M. Buchhold, and S. Diehl, Keldysh field theory for driven open quantum systems, *Rep. Prog. Phys.* **79**, 096001 (2016).
- [110] A. Kamenev, *Field Theory of Non-Equilibrium Systems* (Cambridge University Press, Cambridge, 2011).
- [111] A. Altland and B. Simons, *Condensed Matter Field Theory* (Cambridge University Press, Cambridge, 2006).
- [112] H. J. W. Haug and A.-P. Jauho, *Quantum Kinetics in Transport and Optics of Semiconductors* (Springer, 2008).
- [113] T. Prosen, Third quantization: a general method to solve master equations for quadratic open Fermi systems, *New J. Phys.* **10** 043026 (2008).
- [114] C. E. Bardyn, M. A. Baranov, C. V. Kraus, E. Rico, A. Imamoglu, P. Zoller and S. Diehl, Topology by dissipation, *New J. Phys.* **15** 085001 (2013).
- [115] D. C. Langreth, in *Linear and Nonlinear Electron Transport in Solids*, edited by J. T. Devreese and V. E. VanDoren (Plenum, New York, 1976).
- [116] It is easy to prove that when the Hamiltonian  $\mathbf{H}$ , the loss matrix  $\mathbf{P}$ , and the gain matrix  $\mathbf{Q}$  satisfy inversion symmetry,  $\mathbf{G}_S^R$  and  $\mathbf{G}_S^A$  also satisfy inversion symmetry. Therefore,  $\mathbf{O}$  also corresponds to  $\mathbf{G}_S^R$  and  $\mathbf{G}_S^A$ .
- [117] This conclusion is generally valid; however, as we will discuss later, exceptions arise when the system exhibits non-Hermitian skin effects.
- [118] P. N. Butcher, Thermal and electrical transport formalism for electronic microstructures with many terminals, *J. Phys.: Condens. Matter* **2**, 4869 (1990).
- [119] From the Supplemental Material [108], we see that  $\frac{K}{G} = \mathcal{L}T[1 - \frac{\pi^2}{3}(k_B T)^2(\frac{\tau_1'(\mu)}{\tau_1(\mu)})^2]$ . The Wiedemann-Franz law holds if  $|\frac{\tau_1'(\mu)}{\tau_1(\mu)}| \ll (k_B T)^{-1}$ . In the absence of gain and loss, the values of  $\tau_1'(\mu)$  at the band edges are very large, and  $\tau_1(\mu)$  outside the band is approximately zero. This causes  $|\frac{\tau_1'(\mu)}{\tau_1(\mu)}|$  to become very large, so that  $K/G$  does not satisfy the Wiedemann-Franz law at the band edges and outside the band. However, after the addition of gain and loss, the transmission function  $\tau_1(\mu)$  becomes smooth, ensuring that both at the band edges and outside the band, the Wiedemann-Franz law is satisfied.
- [120] F. Song, S. Yao, and Z. Wang, Non-Hermitian Skin Effect and Chiral Damping in Open Quantum Systems, *Phys. Rev. Lett.* **123**, 170401 (2019).
- [121] C.-H. Liu, K. Zhang, Z. Yang, and S. Chen, Helical damping and dynamical critical skin effect in open quantum systems, *Phys. Rev. Research* **2**, 043167 (2020).
- [122] R. Citro, F. Mancini, *Out-of-equilibrium physics of correlated electron systems* (Springer, 2018).
- [123] K. Yamamoto, N. Hatano, Thermodynamics of the mesoscopic thermoelectric heat engine beyond the linear-response regime, *Phys. Rev. E* **92**, 042165 (2015).
- [124] F. Thompson, A. Kamenev, Field theory of many-body Lindbladian dynamics, *Annals of Physics*, **455**, 169385 (2023).
- [125] Y. Meir, N. S. Wingreen, Landauer formula for the current through an interacting electron region, *Phys. Rev. Lett.* **68**, 2512 (1992).
- [126] D. A. Lavis, B. W. Southern, The inverse of a symmetric banded toepplitz matrix, *Rep. Math. Phys.* **39**, 137 (1997).
- [127] M. Saha, B. K. Agarwalla, M. Kulkarni, A. Purkayastha, Universal Subdiffusive Behavior at Band Edges from Transfer Matrix Exceptional Points, *Phys. Rev. Lett.* **130**, 187101 (2023).

## Supplementary Material: Extended Landauer-Büttiker Formula for Current through Open Quantum Systems with Gain or Loss

In the Supplementary Materials, we first clarify the distinction between Markovian reservoirs and conventional leads, and show the derivation of the Lindblad master equation. We then provide the definition of the current, introduce the Keldysh theory of open fermionic systems, and present the derivation details of the extended Landauer-Büttiker formula. Next, we analytically analyze the effect of inversion symmetry in gain or loss terms on the current using a two-site model, and examine how disorder-induced symmetry breaking leads to current generation. Finally, we study the impact of gain or loss on the Wiedemann-Franz law and investigate the behavior of the current in the presence of the skin effect.

### I. Comparative analysis: Markovian reservoirs and conventional leads

In this section, we clarify the key difference between the Markovian reservoirs responsible for gain and loss and the conventional leads. The system is coupled at both ends to two leads, which serve as particle reservoirs. The particle exchange between the system and the leads constitutes coherent transport, where quantum phase information is preserved. Since the process of particles entering the system from one lead, traversing the system, and exiting into the other lead can be fully described by coherent scattering theory (e.g., Landauer-Büttiker formalism), there is no need to invoke the Lindblad master equation in this case.

In contrast, the gain or loss mechanisms represent incoherent particle exchange with effective Markovian reservoirs. In these processes, quantum coherence (i.e., phase information) is destroyed or no longer tracked. As an intuitive picture, the particles in the system initially possess well-defined coherent phase relations. When a particle escapes into a Markovian reservoir—with no record of its exit time or destination—the coherence among the remaining particles is disrupted. Conversely, a particle injected from the reservoir carries random phase information, further destroying the system's original phase coherence. This memoryless reservoir is not explicitly modeled as a third terminal with a well-defined chemical potential or Fermi distribution. Instead, particle injection and extraction are described by the Lindblad master equation using jump operators, as given in Eq. (3) in the main text:  $L_{1,i} = \sum_j u_{ij} c_j$  and  $L_{2,i} = \sum_j v_{ij} c_j^\dagger$ . These processes are incoherent and irreversible, with no information retained about the origin or destination of the exchanged particles. Only when the reservoir satisfies the Markovian condition can its effects be captured by a Lindblad master equation after tracing out its degrees of freedom (as can be seen in the later derivation). Due to the loss of coherence, the transport behavior of the system cannot be described by coherent scattering theory. Thus, the standard Landauer-Büttiker formula, based on coherent scattering, necessitates modifications and extensions.

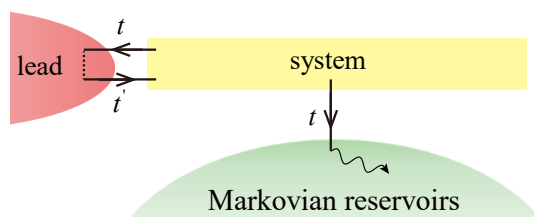


Figure S1: Scheme of particles scatter into the leads and Markovian reservoirs.

The above discussion can be further interpreted as a second-order process, as illustrated in Fig. S1. A particle scatters from the system into the left lead at time  $t$ , propagates within the lead from  $t$  to  $t'$ , and then scatters back into the system. The process can be described by

$$G_S^{(2)}(t, t') \sim g_S^{(0)}(t) \Sigma_{SL} g_L^{(0)}(t - t') \Sigma_{LS} g_S^{(0)}(t'), \quad (\text{S1})$$

where  $g^{(0)}$  denotes the bare Green's function without coupling to leads and reservoirs. We see that it contains the Green's function in the lead  $g_L^{(0)}(t - t')$ , which can be time-dependent and hence carry the memory effect of leads. As a comparison, when a particle scatter into the Markovian reservoir, it will thermalize/dissipate rapidly and lose its initial state information.

## II. Derivation of the Lindblad master equation

In this section, we present the derivation and examine the validity of the Lindblad master equation. For simplicity, we omit the degrees of freedom associated with the leads, as they do not influence the results. The total Hamiltonian of the system, including the Markovian reservoirs, is given by

$$H = H_S + \sum_m [H_B^{(m)} + H_{SB}^{(m)}], \quad (\text{S2})$$

with  $H_S$  represents the Hamiltonian of the central system,  $H_B^{(m)}$  denotes the Hamiltonian of the  $m$ -th reservoir, and  $H_{SB}^{(m)}$  describes the coupling between the central system and the  $m$ -th reservoir. The Hamiltonian of the central system,  $H_S(c_j; c_j^\dagger)$ , is expressed as a function of the annihilation operators ( $c_j$ ) and creation operators ( $c_j^\dagger$ ) at site  $j$ . Each reservoir is modeled as Fermionic (quasi-)particles with the Hamiltonian  $H_B^{(m)} = \sum_k \epsilon_k^m d_k^{(m)\dagger} d_k^{(m)}$ , where  $d_k^{(m)}$  ( $d_k^{(m)\dagger}$ ) denotes the annihilation(creation) operator of  $m$ -th reservoir and  $\epsilon_k^m$  represents its energy. The coupling between central system and the  $m$ -th reservoir is given by

$$H_{SB}^{(m)} = \sum_{jk} [\lambda_{jk}^{(m)} d_k^{(m)\dagger} c_j + \lambda_{jk}^{(m)*} c_j^\dagger d_k^{(m)}]. \quad (\text{S3})$$

where  $\lambda_{jk}^{(m)}$  denotes the coupling strength. It is assumed that the reservoirs satisfy the Markovian condition, meaning the relaxation time  $\tau_B$  of reservoirs is significantly shorter than the dynamical evolution timescale  $\Delta t$  of the central systems [1, 2].

The evolution of density matrix follows the Liouville-von Neumann equation  $\frac{d\rho}{dt} = -i[H, \rho]$ . To facilitate calculations, we adopt the interaction picture:  $\bar{O}(t) = e^{i[H_S + \sum_m H_B^{(m)}]t} O e^{-i[H_S + \sum_m H_B^{(m)}]t}$ . Here  $O$  represents the density matrix  $\rho$  or any operators such as  $c_j$  ( $c_j^\dagger$ ) or  $d_k^{(m)}$  ( $d_k^{(m)\dagger}$ ) in the Schrödinger picture. The coupling term in the interacting picture is expressed as

$$\bar{H}_{SB}^{(m)}(t) = \sum_{jk} [\lambda_{jk}^{(m)} \bar{d}_k^{(m)\dagger}(t) \bar{c}_j(t) + \lambda_{jk}^{(m)*} \bar{c}_j^\dagger(t) \bar{d}_k^{(m)}(t)]. \quad (\text{S4})$$

The Liouville equation in the interacting picture then becomes

$$\frac{d\bar{\rho}(t)}{dt} = -i[\sum_m \bar{H}_{SB}^{(m)}(t), \bar{\rho}(t)]. \quad (\text{S5})$$

Over a time interval  $\Delta t$ , the change in the density matrix  $\Delta\bar{\rho}(t) = \bar{\rho}(t + \Delta t) - \bar{\rho}(t)$  can be calculated by

$$\Delta\bar{\rho}(t) = -i \int_t^{t+\Delta t} dt' [\sum_m \bar{H}_{SB}^{(m)}(t'), \bar{\rho}(t')] - \int_t^{t+\Delta t} dt' \int_t^{t'} dt'' [\sum_m \bar{H}_{SB}^{(m)}(t'), [\sum_n \bar{H}_{SB}^{(n)}(t''), \bar{\rho}(t'')]]. \quad (\text{S6})$$

Assuming the central system and the reservoirs are weak correlated and the reservoirs are in equilibrium, such that then density matrix can be decomposed by  $\bar{\rho}(t) = \bar{\rho}_S(t) \otimes \prod_m \rho_B^{(m)}$ . Substituting it into Eq. (S6) and tracing over the reservoirs gives

$$\Delta\bar{\rho}_S(t) = - \int_t^{t+\Delta t} dt' \int_t^{t'} dt'' Tr_B \left[ \sum_m \bar{H}_{SB}^{(m)}(t'), [\sum_n \bar{H}_{SB}^{(n)}(t''), \bar{\rho}_S(t) \otimes \rho_B] \right]. \quad (\text{S7})$$

Due to the coupling between the system and the reservoir is linear, the term  $\bar{H}_{SB}^{(m)}(t)$  contains odd number of operators  $d^{(m)}$  and  $d^{(m)\dagger}$ , hence  $Tr_B[\bar{H}_{SB}^{(m)}(t), \bar{\rho}(t)] = 0$ . Furthermore, the coarse-grained approximation  $\bar{\rho}(t') \approx \bar{\rho}(t)$  is applied, as  $\bar{\rho}_S$  evolves much slower than the reservoirs. Substituting Eq. (S4) into Eq. (S7) we derive

$$\begin{aligned} \Delta\bar{\rho}_S(t) = & - \int_t^{t+\Delta t} dt' \int_t^{t'} dt'' \sum_{mk} \lambda_{jk}^{(m)*} \lambda_{lk}^{(m)} [\bar{c}_j^\dagger(t') \bar{c}_l(t'') \bar{\rho}_S(t) f_k^{(m)}(t' - t'') - \bar{c}_j^\dagger(t') \bar{\rho}_S(t) \bar{c}_l(t'') h_k^{(m)}(t' - t'') \\ & - \bar{c}_l(t'') \bar{\rho}_S(t) \bar{c}_j^\dagger(t') f_k^{(m)}(t' - t'') + \bar{\rho}_S(t) \bar{c}_l(t'') \bar{c}_j^\dagger(t') h_k^{(m)}(t' - t'')] \\ & + \sum_{mk} \lambda_{jk}^{(m)} \lambda_{lk}^{(m)*} [\bar{c}_j(t') \bar{c}_l^\dagger(t'') \bar{\rho}_S(t) h_k^{(m)*}(t' - t'') - \bar{c}_j(t') \bar{\rho}_S(t) \bar{c}_l^\dagger(t'') f_k^{(m)*}(t' - t'') \\ & - \bar{c}_l^\dagger(t'') \bar{\rho}_S(t) \bar{c}_j(t') h_k^{(m)*}(t' - t'') + \bar{\rho}_S(t) \bar{c}_l^\dagger(t'') \bar{c}_j(t') f_k^{(m)*}(t' - t'')]. \end{aligned} \quad (\text{S8})$$

Here the reservoir correlation functions are

$$f_k^{(m)}(t' - t'') = \text{Tr}_B[\bar{d}_k^{(m)}(t')\bar{d}_k^{(m)\dagger}(t'')\rho_B], \quad h_k^{(m)}(t' - t'') = \text{Tr}_B[\bar{d}_k^{(m)\dagger}(t'')\bar{d}_k^{(m)}(t')\rho_B]. \quad (\text{S9})$$

Considering that  $f_k^{(m)}(\tau)$  and  $h_k^{(m)}(\tau)$  rapidly decay on the timescale  $\tau_B \ll \Delta t$  in the Markovian approximation, we can extend the upper limit of the time integral to infinity. Redefining the variable as  $\tau = t' - t''$ , Eq. (S8) simplifies to

$$\begin{aligned} \Delta \bar{\rho}_S(t) = & - \int_t^{t+\Delta t} dt' \int_0^\infty d\tau \sum_{mk} \lambda_{jk}^{(m)*} \lambda_{lk}^{(m)} [\bar{c}_j^\dagger(t') \bar{c}_l(t') \bar{\rho}_S(t) f_k^{(m)}(\tau) - \bar{c}_j^\dagger(t') \bar{\rho}_S(t) \bar{c}_l(t') h_k^{(m)}(\tau) \\ & - \bar{c}_l(t') \bar{\rho}_S(t) \bar{c}_j^\dagger(t') f_k^{(m)}(\tau) + \bar{\rho}_S(t) \bar{c}_l(t') \bar{c}_j^\dagger(t') h_k^{(m)}(\tau)] \\ & + \sum_{mk} \lambda_{jk}^{(m)} \lambda_{lk}^{(m)*} [\bar{c}_j(t') \bar{c}_l^\dagger(t') \bar{\rho}_S(t) h_k^{(m)*}(\tau) - \bar{c}_j(t') \bar{\rho}_S(t) \bar{c}_l^\dagger(t') f_k^{(m)*}(\tau) \\ & - \bar{c}_l^\dagger(t') \bar{\rho}_S(t) \bar{c}_j(t') h_k^{(m)*}(\tau) + \bar{\rho}_S(t) \bar{c}_l^\dagger(t') \bar{c}_j(t') f_k^{(m)*}(\tau)]. \end{aligned} \quad (\text{S10})$$

Taking the limit  $\Delta t \rightarrow 0$ , we obtain:

$$\begin{aligned} \frac{d\bar{\rho}_S(t)}{dt} = & - \sum_m [\bar{c}_j^\dagger(t) \bar{c}_l(t) \bar{\rho}_S(t) F_{jl}^{(m)} - \bar{c}_j^\dagger(t) \bar{\rho}_S(t) \bar{c}_l(t) H_{jl}^{(m)} - \bar{c}_l(t) \bar{\rho}_S(t) \bar{c}_j^\dagger(t) F_{jl}^{(m)} + \bar{\rho}_S(t) \bar{c}_l(t) \bar{c}_j^\dagger(t) H_{jl}^{(m)}] \\ & - \sum_m [\bar{c}_j(t) \bar{c}_l^\dagger(t) \bar{\rho}_S(t) H_{jl}^{(m)*} - \bar{c}_j(t) \bar{\rho}_S(t) \bar{c}_l^\dagger(t) F_{jl}^{(m)*} - \bar{c}_l^\dagger(t) \bar{\rho}_S(t) \bar{c}_j(t) H_{jl}^{(m)*} + \bar{\rho}_S(t) \bar{c}_l^\dagger(t) \bar{c}_j(t) F_{jl}^{(m)*}]. \end{aligned} \quad (\text{S11})$$

Here,

$$F_{jl}^{(m)} = \sum_k \lambda_{jk}^{(m)*} \lambda_{lk}^{(m)} \int_0^\infty d\tau f_k^{(m)}(\tau), \quad H_{jl}^{(m)} = \sum_k \lambda_{jk}^{(m)} \lambda_{lk}^{(m)*} \int_0^\infty d\tau h_k^{(m)}(\tau). \quad (\text{S12})$$

Separating  $F$  and  $H$  into Hermitian and anti-Hermitian parts as  $F = \bar{F} + i\tilde{F}$  and  $H = \bar{H} + i\tilde{H}$ , and together with Eq. (S11) we arrive at

$$\begin{aligned} \frac{d\bar{\rho}_S(t)}{dt} = & -i \left[ \sum_{mjl} \bar{F}_{jl}^{(m)} \bar{c}_j^\dagger(t) \bar{c}_l(t) + \sum_{mjl} \tilde{H}_{jl}^{(m)} \bar{c}_l(t) \bar{c}_j^\dagger(t), \bar{\rho}_S(t) \right] \\ & + \sum_{mjl} \bar{F}_{jl}^{(m)} [2\bar{c}_l(t) \bar{\rho}_S(t) \bar{c}_j^\dagger(t) - \{\bar{c}_j^\dagger(t) \bar{c}_l(t), \bar{\rho}_S(t)\}] + \sum_{mjl} \bar{H}_{jl}^{(m)} [2\bar{c}_j^\dagger(t) \bar{\rho}_S(t) \bar{c}_l(t) - \{\bar{c}_l(t) \bar{c}_j^\dagger(t), \bar{\rho}_S(t)\}]. \end{aligned} \quad (\text{S13})$$

Transforming back into the Schrödinger picture via  $\frac{d\bar{\rho}_S(t)}{dt} = e^{iH_S t} \left( \frac{d\rho_S}{dt} + i[H_S, \rho_S] \right) e^{-iH_S t}$ , we obtain the Lindblad equation:

$$\frac{d\rho_S}{dt} = -i[H_S + H_{Lamb}, \rho_S] + \sum_{\nu=1,2} \sum_{m,k} (2L_{\nu,mk} \rho_S L_{\nu,mk}^\dagger - \{L_{\nu,mk}^\dagger L_{\nu,mk}, \rho_S\}), \quad (\text{S14})$$

where the Lamb shift Hamiltonian is given by  $H_{Lamb} = \sum_{mjl} (\bar{F}_{jl}^{(m)} c_j^\dagger c_l + \tilde{H}_{jl}^{(m)} c_l c_j^\dagger)$ , and the Lindblad operators

$$L_{1,mk} = \sum_j \lambda_{jk}^{(m)} \sqrt{\text{Re} \int_0^\infty d\tau f_k^{(m)}(\tau)} c_j, \quad L_{2,mk} = \sum_j \lambda_{jk}^{(m)*} \sqrt{\text{Re} \int_0^\infty d\tau h_k^{(m)}(\tau)} c_j^\dagger, \quad (\text{S15})$$

Hence each energy level  $\epsilon_k$  in the  $m$ th reservoir can be described by two Lindblad dissipators  $L_{1,mk}$  and  $L_{2,mk}$ , controlling the particle loss and gain. In general, the reservoir correlation functions can generally be expressed as:

$$f_k^{(m)}(\tau) = e^{-\left(i\epsilon_k + \frac{1}{\tau_k^{(m)}}\right)\tau} (1 - n_k^{(m)}), \quad h_k^{(m)}(\tau) = e^{-\left(i\epsilon_k + \frac{1}{\tau_k^{(m)}}\right)\tau} n_k^{(m)}, \quad (\text{S16})$$

where  $\tau_k^{(m)}$  represents the (quasi-)particle's lifetime, and  $n_k^{(m)} = \text{Tr}_B[d_k^{(m)\dagger} d_k^{(m)} \rho_B]$  denotes the particle number in equilibrium. Integral over  $\tau$  we get  $\int_0^\infty d\tau f_k^{(m)}(\tau) = \frac{\tau_k^{(m)} - i\epsilon_k \tau_k^{(m)2}}{1 + \epsilon_k^2 \tau_k^{(m)2}} (1 - n_k^{(m)})$  and  $\int_0^\infty d\tau h_k^{(m)}(\tau) = \frac{\tau_k^{(m)} - i\epsilon_k \tau_k^{(m)2}}{1 + \epsilon_k^2 \tau_k^{(m)2}} n_k^{(m)}$ .

Hence Eq. (S15) can be simplified to

$$L_{1,mk} = \sum_j \lambda_{jk}^{(m)} \sqrt{\frac{\tau_k^{(m)}(1 - n_k^{(m)})}{1 + \epsilon_k^2 \tau_k^{(m)2}}} c_j, \quad L_{2,mk} = \sum_j \lambda_{jk}^{(m)*} \sqrt{\frac{\tau_k^{(m)} n_k^{(m)}}{1 + \epsilon_k^2 \tau_k^{(m)2}}} c_j^\dagger. \quad (\text{S17})$$

In the continuous limit, it is convenient to define the local spectral density of the  $m$ th reservoir  $J_{jl}^{(m)} = \sum_k \lambda_{jk}^{(m)*} \lambda_{lk}^{(m)} \delta(\omega - \epsilon_k^m)$ , then we have  $\bar{F}_{jl}^{(m)} = \int d\omega J_{jl}^{(m)}(\omega) \frac{\tau_\omega^{(m)}(1-n_\omega^{(m)})}{1+\omega^2\tau_\omega^{(m)2}}$  and  $\bar{H}_{jl}^{(m)} = \int d\omega J_{jl}^{(m)}(\omega) \frac{\tau_\omega^{(m)}n_\omega^{(m)}}{1+\omega^2\tau_\omega^{(m)2}}$ . The Lindblad equation Eq. (S14) becomes

$$\frac{d\rho_S}{dt} = -i[H_S + H_{Lamb}, \rho_S] + \sum_m \bar{F}_{jl}^{(m)} (2c_l \rho_S c_j^\dagger - \{c_j^\dagger c_l, \rho_S\}) + \sum_m \bar{H}_{jl}^{(m)} (2c_j^\dagger \rho_S c_l - \{c_l c_j^\dagger, \rho_S\}). \quad (\text{S18})$$

Noting that  $\bar{\mathbf{F}}^{(m)}$  and  $\bar{\mathbf{H}}^{(m)}$  are Hermitian, positive semi-definite matrices. Their summations are diagonalized by  $\mathbf{U} \sum_m \bar{\mathbf{F}}^{(m)} \mathbf{U}^\dagger = \text{diag}(x_{m,1}^2, x_{m,2}^2, \dots)$  and  $\mathbf{V} \sum_m \bar{\mathbf{H}}^{(m)} \mathbf{V}^\dagger = \text{diag}(y_{m,1}^2, y_{m,2}^2, \dots)$ , hence Eq. (S18) can be further simplified to

$$\frac{d\rho_S}{dt} = -i[H_S + H_{Lamb}, \rho_S] + \sum_{\nu=1,2} \sum_m (2L_{\nu,m} \rho_S L_{\nu,m}^\dagger - \{L_{\nu,m}^\dagger L_{\nu,m}, \rho_S\}), \quad (\text{S19})$$

with Lindblad operators

$$L_{1,m} = \sum_j x_m U_{mj} c_j, \quad L_{2,m} = \sum_j y_m V_{mj}^* c_j^\dagger. \quad (\text{S20})$$

By comparing Eq. (S20) with Eq. (3) in the main text, we identify  $u_{mj} = x_m U_{mj}$  and  $v_{mj} = y_m V_{mj}^*$ .

The Lamb shift term  $H_{Lamb}$  originates from the imaginary part of the reservoir correlation functions and accounts for energy renormalization due to virtual transitions between the system and the reservoir. In most practical cases, this contribution is negligibly small for the following reasons. First, the Lamb shift appears only at second order and is typically much smaller than the coherent system energy scales. Second, we are primarily interested in dissipative dynamics, where the non-unitary evolution governed by the Lindblad terms dominates, and we are not concerned with the small energy renormalizations induced by dissipation. Third, under the Markov approximation (where reservoir modes have very short lifetimes), the rapid decay of correlation functions causes their oscillatory components to average out:  $\text{Im} \int_0^\infty f_k(\tau) d\tau \rightarrow \tau_B^2 \rightarrow 0$ , since the imaginary part cannot accumulate under fast exponential damping. In addition, system-reservoir coupling is often local in space, such that only the diagonal elements ( $j = l$ ) of  $H_{Lamb}$  contribute, leading to a weak on-site energy shift. In these circumstances, the Lamb shift has little to no observable impact on the dissipative dynamics of the system and can be safely neglected in the analysis.

Moreover, from the expressions of the gain and loss terms in Eq. (S17), we can identify the key factors that influence their strength and form. 1. The lifetime of the reservoir mode  $\tau_k$ . 2. The occupation number of the reservoir mode  $n_k$ : The loss channel scales as  $L_1 \propto \sqrt{1-n_k}$ , indicating that the reservoir must be partially empty ( $n_k \neq 1$ ) to accept particles from the system. The gain channel scales as  $L_2 \propto \sqrt{n_k}$ , meaning that the reservoir must be partially occupied ( $n_k \neq 0$ ) in order to inject particles into the system. When  $n_k = 1$ , only gain occurs; when  $n_k = 0$ , only loss occurs; and for  $0 < n_k < 1$ , both gain and loss processes are possible. 3. The energy detuning of the reservoir mode  $\epsilon_k$ : When the reservoir mode energy approaches the system energy levels (i.e., smaller  $\epsilon_k$ ), the strength of gain and loss increases due to enhanced resonance. 4. The coupling strength and type between system and reservoir  $\lambda_{jk}$ :  $\lambda_{jk}$  directly determines the strength and specific form of the Lindblad operators. In the expressions for  $L_1$  and  $L_2$ , the summation involves  $\lambda_{jk}$ , which contains information about the index  $j$ . Therefore, it determines whether the gain or loss is on-site, bond-related, or involves lattice sites at greater distances.

### III. Definition of particle and energy currents

The steady state of the system we study (Fig. 1 in the main text) is not in equilibrium, which leads to difficulties in defining the global thermodynamic variables. To overcome this problem, it is convenient to instead study the particle and energy flows in the lead [3]. From the first law of thermodynamics, we have

$$dU_{L(R)} = dQ_{L(R)} + dW_{L(R)}, \quad (\text{S21})$$

where  $U_{L(R)} = \langle H_{L(R)} \rangle$  is the energy of  $L(R)$ -lead,  $dU_{L(R)}$  and  $dQ_{L(R)}$  are the energy and heat flowing into the  $L(R)$ -lead, and  $dW_{L(R)} = \mu_{L(R)} d\mathcal{N}_{L(R)}$ , with  $\mathcal{N}_{L(R)}$  being the particle number of the  $L(R)$ -lead, is the work done on the  $L(R)$ -lead. Typically, the voltage  $V$  is defined as the difference of chemical potential,  $eV = \mu_R - \mu_L$ . The particle and energy currents are then defined as

$$J_L^0 = -\frac{d\mathcal{N}_L}{dt}, \quad J_R^0 = \frac{d\mathcal{N}_R}{dt}, \quad J_L^1 = -\frac{dU_L}{dt}, \quad J_R^1 = \frac{dU_R}{dt}. \quad (\text{S22})$$

Substituting into Eq. (S21), we see that the heat current is

$$J_L^Q = -\frac{dQ_L}{dt} = J_L^1 - \mu_L J_L^0, \quad J_R^Q = \frac{dQ_R}{dt} = J_R^1 - \mu_R J_R^0. \quad (\text{S23})$$

It is common to study the net current  $J$  defined by

$$J^{0/1/Q} = \frac{1}{2}(J_L^{0/1/Q} + J_R^{0/1/Q}). \quad (\text{S24})$$

#### IV. Keldysh theory of open fermionic systems

In a system coupled with the environment, one often studies the reduced density matrix  $\rho$ . Under the Markovian approximation, the evolution of  $\rho$  can be described by the Lindblad master equation

$$\frac{d\rho}{dt} = -i[H, \rho] + \sum_m (2L_m \rho L_m^\dagger - \{L_m^\dagger L_m, \rho\}). \quad (\text{S25})$$

Here,  $H$  is the Hamiltonian (renormalized by the environment), and  $L_m$  are the quantum jump operators describing the coupling between the system and the environment. It is convenient to introduce the Lindblad-Keldysh partition function,  $Z = \text{Tr}[\rho(t)]$ , which is always equal to one due to the normalization of the density matrix. By inserting fermionic coherent states  $|\psi\rangle$ , which are eigenstates of the annihilation operators:  $c_j|\psi\rangle = \psi_j|\psi\rangle$ , the partition function can be written as  $Z = \int D[\bar{\psi}^\pm, \psi^\pm] e^{i\mathcal{S}}$  [4, 5], where the superscript  $\pm$  denotes the indices of Keldysh contour, and the action reads

$$\mathcal{S} = \int dt [\sum_j (\bar{\psi}_j^+ i\partial_t \psi_j^+ - \bar{\psi}_j^- i\partial_t \psi_j^-) - i\mathcal{L}]. \quad (\text{S26})$$

Here, the Liouvillian  $\mathcal{L} = -iH^+ + iH^- - (L^\dagger L)^+ - (L^\dagger L)^- + 2(L)^+(L^\dagger)^-$ , where  $H^\pm$  and  $L^\pm$  satisfy:  $O^+ = \frac{\langle \psi^+(t_{n+1})|O|\psi^+(t_n)\rangle}{\langle \psi^+(t_{n+1})|\psi^+(t_n)\rangle}$  and  $O^- = \frac{\langle -\psi^-(t_n)|O|-\psi^-(t_{n+1})\rangle}{\langle -\psi^-(t_n)|-\psi^-(t_{n+1})\rangle}$ , with  $O$  representing  $H$  or  $L$ . The description in this basis often contains redundancy. To eliminate this redundancy and facilitate calculations, a Keldysh rotation is usually performed,

$$\begin{cases} \psi^1 = \frac{1}{\sqrt{2}}(\psi^+ + \psi^-), & \bar{\psi}^1 = \frac{1}{\sqrt{2}}(\bar{\psi}^+ - \bar{\psi}^-), \\ \psi^2 = \frac{1}{\sqrt{2}}(\psi^+ - \psi^-), & \bar{\psi}^2 = \frac{1}{\sqrt{2}}(\bar{\psi}^+ + \bar{\psi}^-). \end{cases} \quad (\text{S27})$$

Hence, the Liouvillian and action can be expressed as functions of  $\bar{\psi}^{1,2}$  and  $\psi^{1,2}$ .

Suppose the Hamiltonian is non-interacting and the Lindbladian is linear,

$$H = \sum_{jk} h_{jk} c_j^\dagger c_k, \quad L_{1,j} = \sum_k u_{jk} c_k, \quad L_{2,j} = \sum_k v_{jk} c_k^\dagger. \quad (\text{S28})$$

The action is quadratic and can be written in matrix form in Keldysh space:

$$\mathcal{S} = \int dt (\bar{\psi}^1 \quad \bar{\psi}^2) \begin{pmatrix} i\partial_t - \mathbf{h} + i\mathbf{P} + i\mathbf{Q} & -2i(\mathbf{Q} - \mathbf{P}) \\ 0 & i\partial_t - \mathbf{h} - i\mathbf{P} - i\mathbf{Q} \end{pmatrix} \begin{pmatrix} \psi^1 \\ \psi^2 \end{pmatrix}, \quad (\text{S29})$$

where the matrix element of the loss matrix  $\mathbf{P}$  is  $P_{jk} = \sum_m u_{mj}^* u_{mk}$ , and the matrix element of the gain matrix  $\mathbf{Q}$  is  $Q_{jk} = \sum_m v_{mj} v_{mk}^*$ . It is convenient to define the damping matrix  $\mathbf{X} = \mathbf{h} - i\mathbf{P} - i\mathbf{Q}$  and the imbalance matrix  $\mathbf{Y} = 2(\mathbf{P} - \mathbf{Q})$ . The Green's functions can be derived by inverting the action matrix  $\mathbf{S}$ , i.e.,

$$\begin{pmatrix} \mathbf{g}_{jk}^{\mathcal{R}} & \mathbf{g}_{jk}^{\mathcal{K}} \\ 0 & \mathbf{g}_{jk}^{\mathcal{A}} \end{pmatrix} = \begin{pmatrix} i\partial_t - \mathbf{X} & i\mathbf{Y} \\ 0 & i\partial_t - \mathbf{X}^\dagger \end{pmatrix}^{-1}. \quad (\text{S30})$$

If we focus on the steady state, the Green's function depends only on the time difference  $t - t'$ . Hence, the explicit expressions of the Green's functions in the frequency domain are

$$\mathbf{g}^{\mathcal{R}} = \frac{1}{\omega - \mathbf{X}}, \quad \mathbf{g}^{\mathcal{A}} = \frac{1}{\omega - \mathbf{X}^\dagger}, \quad \mathbf{g}^{\mathcal{K}} = -\frac{1}{\omega - \mathbf{X}} i\mathbf{Y} \frac{1}{\omega - \mathbf{X}^\dagger}. \quad (\text{S31})$$

We see that the retarded and advanced Green's functions contain only the spectral information of the damping matrix, while the Keldysh Green's function, which captures the particle distribution in the steady state, contains both the spectral information of  $\mathbf{X}$  and the imbalance matrix  $\mathbf{Y}$ . By using the identities  $\mathbf{g}^> = \frac{1}{2}(\mathbf{g}^{\mathcal{K}} + \mathbf{g}^{\mathcal{R}} - \mathbf{g}^{\mathcal{A}})$  and  $\mathbf{g}^< = \frac{1}{2}(\mathbf{g}^{\mathcal{K}} - \mathbf{g}^{\mathcal{R}} + \mathbf{g}^{\mathcal{A}})$ , the steady-state greater and lesser Green's functions can be derived

$$\mathbf{g}^> = -2i\mathbf{g}^{\mathcal{R}}\mathbf{P}\mathbf{g}^{\mathcal{A}}, \quad \mathbf{g}^< = 2i\mathbf{g}^{\mathcal{R}}\mathbf{Q}\mathbf{g}^{\mathcal{A}}. \quad (\text{S32})$$

We can see that the greater Green's function is directly proportional to the loss matrix  $\mathbf{P}$  and the lesser Green's function is directly proportional to the gain matrix  $\mathbf{Q}$ .

### V. Derivation details of extended Landauer-Büttiker formula

Suppose the full Hamiltonian of the system shown in Fig. 1 of the main text is

$$H = H_S + H_L + H_R + (H_{SL} + H_{SR} + h.c.), \quad (\text{S33})$$

where  $H_S$  is the Hamiltonian of the central system,  $H_{L(R)}$  are the Hamiltonians of left (right) leads, and  $H_{SL(SR)}$  represents the coupling between the central system and the left (right) lead. We assume that the Markovian reservoirs only interact with the central system, and hence the Lindblad operators  $L_m$  contain only the operators acting on the central system. The explicit form of the Hamiltonian in Eq. (S33) is

$$\begin{aligned} H_S &= \sum_{ij} h_{S,ij} c_i^\dagger c_j, & H_L &= \sum_k \epsilon_{L,k} d_{L,k}^\dagger d_{L,k}, & H_R &= \sum_k \epsilon_{R,k} d_{R,k}^\dagger d_{R,k}, \\ H_{LS} &= \sum_{kj} t_{L,kj} d_{L,k}^\dagger c_j, & H_{RS} &= \sum_{kj} t_{R,kj} d_{R,k}^\dagger c_j. \end{aligned} \quad (\text{S34})$$

Here  $c_j(c_j^\dagger)$  is the annihilation (creation) operator on the  $j$ -th lattice site of the central system, and  $d_{L(R),k}(d_{L(R),k}^\dagger)$  is the annihilation (creation) operator on the momentum  $k$  of the left (right) lead. We first consider the current flowing out of the left lead, as shown in Eq. (S22), which can be calculated by

$$\begin{aligned} J_L^0 &= -\frac{d\mathcal{N}_L}{dt} = -\frac{i}{\hbar}[H, \mathcal{N}_L] = \frac{1}{\hbar} \sum_k (t_{L,kj} G_{SL,jk}^< - t_{L,kj}^* G_{LS,kj}^<), \\ J_L^1 &= -\frac{dU_L}{dt} = -\frac{i}{\hbar}[H, U_L] = \frac{1}{\hbar} \sum_k \epsilon_{L,k} (t_{L,kj} G_{SL,jk}^< - t_{L,kj}^* G_{LS,kj}^<), \end{aligned} \quad (\text{S35})$$

Here, the particle number operator is  $\mathcal{N}_L = \sum_k d_{L,k}^\dagger d_{L,k}$  and the energy is  $U_L = \sum_k \epsilon_{L,k} d_{L,k}^\dagger d_{L,k}$ . To derive this equation, we used the Heisenberg equation of motion for operators, which is valid here because the leads are assumed to be uncoupled from the reservoir. In a more general scenario where the reservoir is coupled to both the central system and the leads, one would instead use the Lindblad equation for operators. In the following, we use  $\mathbf{g}$  to denote the bare Green's function (i.e., the Green's function without coupling to the leads), and  $\mathbf{G}$  to denote the full Green's functions. By applying the Langreth theorem, one can obtain

$$\begin{aligned} \mathbf{G}_{LS}^< &= \mathbf{g}_L^< \mathbf{\Sigma}_{LS}^{\mathcal{A}} \mathbf{G}_S^{\mathcal{A}} + \mathbf{g}_L^{\mathcal{R}} \mathbf{\Sigma}_{LS}^{\mathcal{R}} \mathbf{G}_S^< + \mathbf{g}_L^{\mathcal{R}} \mathbf{\Sigma}_L^< \mathbf{G}_{LS}^{\mathcal{A}}, \\ \mathbf{G}_{SL}^< &= \mathbf{G}_S^< \mathbf{\Sigma}_{SL}^{\mathcal{A}} \mathbf{g}_L^{\mathcal{A}} + \mathbf{G}_S^{\mathcal{R}} \mathbf{\Sigma}_{SL}^{\mathcal{R}} \mathbf{g}_L^< + \mathbf{G}_{SL}^{\mathcal{R}} \mathbf{\Sigma}_L^< \mathbf{g}_L^{\mathcal{A}}. \end{aligned} \quad (\text{S36})$$

and

$$\begin{aligned} \mathbf{G}_S^< &= \mathbf{g}_S^< + (\mathbf{g}_S^< \mathbf{\Sigma}_{SL}^{\mathcal{A}} \mathbf{G}_{LS}^{\mathcal{A}} + \mathbf{g}_S^{\mathcal{R}} \mathbf{\Sigma}_{SL}^{\mathcal{R}} \mathbf{G}_{LS}^< + \mathbf{g}_S^{\mathcal{R}} \mathbf{\Sigma}_{SL}^< \mathbf{G}_{LS}^{\mathcal{A}} + L \leftrightarrow R), \\ \mathbf{G}_S^> &= \mathbf{g}_S^> + (\mathbf{g}_S^> \mathbf{\Sigma}_{SL}^{\mathcal{A}} \mathbf{G}_{LS}^{\mathcal{A}} + \mathbf{g}_S^{\mathcal{R}} \mathbf{\Sigma}_{SL}^{\mathcal{R}} \mathbf{G}_{LS}^> + \mathbf{g}_S^{\mathcal{R}} \mathbf{\Sigma}_{SL}^> \mathbf{G}_{LS}^{\mathcal{A}} + L \leftrightarrow R). \end{aligned} \quad (\text{S37})$$

Here,  $\mathbf{\Sigma}_L^<$  vanishes for non-interacting, non-dissipating leads. In equilibrium, the bare Green's functions of the left lead are

$$g_{L,k}^< = 2\pi i f_L \delta(\omega - \epsilon_{L,k}), \quad g_{L,k}^> = 2\pi i (f_L - 1) \delta(\omega - \epsilon_{L,k}), \quad (\text{S38})$$

where  $f_L = \frac{1}{e^{(\omega - \mu_L)/k_B T_L + 1}}$  is the Fermi distribution. Transforming into the frequency domain,  $G(t - t') = \int \frac{d\omega}{2\pi} e^{-i\frac{\omega(t-t')}{\hbar}} G(\omega)$ , and substituting Eq. (S36) and (S38) into Eq. (S35), we get

$$J_L^\lambda = \frac{i}{\hbar} \int \frac{d\omega}{2\pi} \omega^\lambda \text{Tr}[f_L \Gamma_L (\mathbf{G}_S^{\mathcal{R}} - \mathbf{G}_S^{\mathcal{A}}) + \Gamma_L \mathbf{G}_S^<]. \quad (\text{S39})$$

Here,  $\lambda = 0, 1$ , and the spectral density is  $\Gamma_L = i(\tilde{\Sigma}_L^{\mathcal{R}} - \tilde{\Sigma}_L^{\mathcal{A}})$ , with the leads-induced self-energies  $\tilde{\Sigma}_L^{\mathcal{R}} = \Sigma_{SL}^{\mathcal{R}} \mathbf{g}_L^{\mathcal{R}} \Sigma_{LS}^{\mathcal{R}}$ , and  $\tilde{\Sigma}_L^{\mathcal{A}} = \Sigma_{SL}^{\mathcal{A}} \mathbf{g}_L^{\mathcal{A}} \Sigma_{LS}^{\mathcal{A}}$ . The expression for  $J_R^\lambda$  can be derived in the same way. Substituting  $J_L^\lambda$  and  $J_R^\lambda$  into Eq. (S24), the current  $J^\lambda$  can be written as

$$J^\lambda = \frac{i}{2\hbar} \int \frac{d\omega}{2\pi} \omega^\lambda \text{Tr}[(f_L \Gamma_L - f_R \Gamma_R) (\mathbf{G}_S^{\mathcal{R}} - \mathbf{G}_S^{\mathcal{A}}) + (\Gamma_L - \Gamma_R) \mathbf{G}_S^<]. \quad (\text{S40})$$

This formula applies to a general many-body Hamiltonian and Lindbladian. It can be seen that all the information about dissipation is contained in the Green's function  $\mathbf{G}_S$ . In the absence of dissipation, Eq. (S40) reduces to the Meir-Wingreen formula [6]. By multiplying  $\omega - \mathbf{X}$  from the left of  $\mathbf{G}_S^<(\mathbf{G}_S^>)$  in Eq. (S37) and using the identities in Eq. (S32), we obtain

$$\begin{aligned} \mathbf{G}_S^< &= \mathbf{G}_S^{\mathcal{R}} (\Sigma_{SL}^{\mathcal{R}} \mathbf{g}_L^< \Sigma_{LS}^{\mathcal{A}} + \Sigma_{SR}^{\mathcal{R}} \mathbf{g}_R^< \Sigma_{RS}^{\mathcal{A}} + 2i\mathbf{Q}) \mathbf{G}_S^{\mathcal{A}}, \\ \mathbf{G}_S^> &= \mathbf{G}_S^{\mathcal{R}} (\Sigma_{SL}^{\mathcal{R}} \mathbf{g}_L^> \Sigma_{LS}^{\mathcal{A}} + \Sigma_{SR}^{\mathcal{R}} \mathbf{g}_R^> \Sigma_{RS}^{\mathcal{A}} - 2i\mathbf{P}) \mathbf{G}_S^{\mathcal{A}}, \end{aligned} \quad (\text{S41})$$

where we assume no dissipation in the leads, such that  $\Sigma_{SL}^{\mathcal{R}} = \Sigma_{SR}^{\mathcal{R}} = 0$ . Then, noting that  $\Sigma_{SL(R)}^{\mathcal{R}} \mathbf{g}_{L(R)}^< \Sigma_{L(R)S}^{\mathcal{A}} = if_{L(R)} \Gamma_{L(R)}$  and  $\Sigma_{SL(R)}^{\mathcal{R}} \mathbf{g}_{L(R)}^> \Sigma_{L(R)S}^{\mathcal{A}} = i(f_{L(R)} - 1) \Gamma_{L(R)}$ , we finally obtain

$$\begin{aligned} \mathbf{G}_S^< &= i\mathbf{G}_S^{\mathcal{R}} (f_L \Gamma_L + f_R \Gamma_R + 2\mathbf{Q}) \mathbf{G}_S^{\mathcal{A}}, \\ \mathbf{G}_S^> &= i\mathbf{G}_S^{\mathcal{R}} (f_L \Gamma_L + f_R \Gamma_R - \Gamma_L - \Gamma_R - 2\mathbf{P}) \mathbf{G}_S^{\mathcal{A}}. \end{aligned} \quad (\text{S42})$$

where  $\mathbf{G}_S^{\mathcal{R}} = (\mathbf{G}_S^{\mathcal{A}})^\dagger = [(\mathbf{g}_S^{\mathcal{R}})^{-1} - \tilde{\Sigma}_L^{\mathcal{R}} - \tilde{\Sigma}_R^{\mathcal{R}}]^{-1}$ , and  $(\mathbf{g}_S^{\mathcal{R}})^{-1} = \omega - \mathbf{h}_S + i\mathbf{P} + i\mathbf{Q}$ . Substituting Eq. (S42) into Eq. (S40) and using the identity  $\mathbf{G}_S^{\mathcal{R}} - \mathbf{G}_S^{\mathcal{A}} = \mathbf{G}_S^> - \mathbf{G}_S^<$ , the current can be written in a simple form

$$J^\lambda = J_{LR}^\lambda + J_{LS}^\lambda - J_{RS}^\lambda, \quad (\text{S43})$$

with

$$\begin{aligned} J_{LR}^\lambda &= \int \frac{d\omega}{2\hbar} (f_L - f_R) \omega^\lambda \text{Tr}[\Gamma_L \mathbf{G}_S^{\mathcal{R}} \Gamma_R \mathbf{G}_S^{\mathcal{A}} + \Gamma_R \mathbf{G}_S^{\mathcal{R}} \Gamma_L \mathbf{G}_S^{\mathcal{A}}], \\ J_{LS}^\lambda &= \int \frac{d\omega}{\hbar} f_L \omega^\lambda \text{Tr}[\Gamma_L \mathbf{G}_S^{\mathcal{R}} \mathbf{P} \mathbf{G}_S^{\mathcal{A}}] + \int \frac{d\omega}{\hbar} (f_L - 1) \omega^\lambda \text{Tr}[\Gamma_L \mathbf{G}_S^{\mathcal{R}} \mathbf{Q} \mathbf{G}_S^{\mathcal{A}}], \\ J_{RS}^\lambda &= \int \frac{d\omega}{\hbar} f_R \omega^\lambda \text{Tr}[\Gamma_R \mathbf{G}_S^{\mathcal{R}} \mathbf{P} \mathbf{G}_S^{\mathcal{A}}] + \int \frac{d\omega}{\hbar} (f_R - 1) \omega^\lambda \text{Tr}[\Gamma_R \mathbf{G}_S^{\mathcal{R}} \mathbf{Q} \mathbf{G}_S^{\mathcal{A}}]. \end{aligned} \quad (\text{S44})$$

Here, the Landauer term  $J_{LR}^\lambda$  describes the current flow from the left lead to the right lead directly, and  $J_{LS}^\lambda - J_{RS}^\lambda$  represents the current flow from the left lead to the right lead through the reservoirs.

Though Eq. (S43) gives clear physical origin for the steady-state current, it is more convenient to separate the current into

$$J^\lambda = J_0^\lambda + \delta J_1^\lambda, \quad (\text{S45})$$

where the reference current  $J_0^\lambda$  represents the net current if both leads are at the same chemical potential and temperature. The response current  $\delta J_1^\lambda$  captures the change in current induced by a chemical potential and temperature gradient. Suppose the chemical potential and temperature gradient are applied to the left lead, i.e.,  $\mu_R = \mu$ ,  $T_R = T$ ,  $f_R = f$ , and  $\mu_L = \mu_R + \delta\mu$ ,  $T_L = T_R + \delta T$ ,  $f_L = f_R + \delta f$ . Then, we can derive

$$J_0^\lambda = \int \frac{d\omega}{\hbar} \omega^\lambda f(\omega) \tau_{0,l}(\omega) + \int \frac{d\omega}{\hbar} \omega^\lambda (f(\omega) - 1) \tau_{0,g}(\omega), \quad \delta J_1^\lambda = \int \frac{d\omega}{\hbar} \omega^\lambda \delta f(\omega) \tau_1(\omega), \quad (\text{S46})$$

where the transmission function from the loss channels is  $\tau_{0,l}(\omega) = \text{Tr}[(\Gamma_L - \Gamma_R) \mathbf{G}_S^{\mathcal{R}} \mathbf{P} \mathbf{G}_S^{\mathcal{A}}]$ , the transmission function from the gain channels is  $\tau_{0,g}(\omega) = \text{Tr}[(\Gamma_L - \Gamma_R) \mathbf{G}_S^{\mathcal{R}} \mathbf{Q} \mathbf{G}_S^{\mathcal{A}}]$ , and the transmission function  $\tau_1$  is  $\tau_1(\omega) = \text{Tr}[\frac{1}{2} \Gamma_L \mathbf{G}_S^{\mathcal{R}} \Gamma_R \mathbf{G}_S^{\mathcal{A}} + \frac{1}{2} \Gamma_R \mathbf{G}_S^{\mathcal{R}} \Gamma_L \mathbf{G}_S^{\mathcal{A}} + \Gamma_L \mathbf{G}_S^{\mathcal{R}} (\mathbf{P} + \mathbf{Q}) \mathbf{G}_S^{\mathcal{A}}]$ .

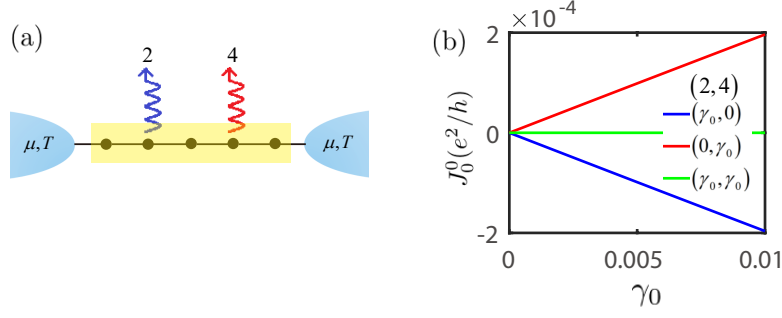


Figure S2: (a) Scheme of a five-site system with local monitoring. (b) The current  $J_0^0$  as a function of monitoring strength  $\gamma_0$ . The blue and red lines represent monitoring at the second and fourth site, respectively; the green line corresponds to monitoring at the second and fourth sites situationally.

## VI. Effect of inversion symmetry in gain or loss terms on the current: a two-site example

In the main text, we have mentioned that when there is no chemical potential or temperature difference between the leads, the breaking of inversion symmetry in the gain or loss terms, or in the system, can lead to the generation of current. Consider a two-site example with Hamiltonian  $H_S = -(c_1^\dagger c_2 + c_2^\dagger c_1)$ . The local on-site monitoring is described by Lindblad operators  $L_1 = \sqrt{\gamma_1}c_1$  and  $L_2 = \sqrt{\gamma_2}c_2$ . The leads self-energies  $(\tilde{\Sigma}_L^R)_{11} = (\tilde{\Sigma}_R^R)_{NN} = -\frac{i\Gamma}{2}$  are constants in the wide-band limit. The particle current in Eq. (S45) is  $J_0^0 = \Gamma \int \frac{d\omega}{h} f(\omega) \tau_{0,l}(\omega)$  with

$$\tau_{0,l}(\omega) = \frac{\gamma_1(|\omega + i\gamma_2 + \frac{i\Gamma}{2}|^2 - 1) - \gamma_2(|\omega + i\gamma_1 + \frac{i\Gamma}{2}|^2 - 1)}{(|\omega + i\gamma_1 + \frac{i\Gamma}{2}|^2 - 1)(|\omega + i\gamma_2 + \frac{i\Gamma}{2}|^2 - 1)}. \quad (\text{S47})$$

Now consider the situation where the monitoring strength is very small, i.e.,  $\gamma_1, \gamma_2 \ll \omega$ . Then, Eq. (S47) can be simplified to

$$\tau_{0,l}(\omega) \approx (\gamma_1 - \gamma_2) \frac{|\omega + \frac{i\Gamma}{2}|^2 - 1}{|\omega + \frac{i\Gamma}{2}|^2 - 1}. \quad (\text{S48})$$

As a result,  $J_0^0 \propto \gamma_1 - \gamma_2$  for weak  $\gamma_1$  and  $\gamma_2$ , and in the presence of inversion symmetry, where  $\gamma_1 = \gamma_2$ , the current  $J_0^0$  vanishes, as shown in Fig. 2(b2) in the main text.

Numerically, we checked that the results can be generalized to the model with more sites. Fig. ?? shows an example with five sites. Similar to the  $N = 2$  case, the current  $J_0^0$  is proportional to  $\gamma_0$  for small monitoring at the second or fourth site. However, the current vanishes when measuring at the second and fourth sites due to inversion symmetry. It can be verified that adding gain or loss terms at more sites leads to the same conclusion: the presence or absence of inversion symmetry causes the current to vanish or emerge.

## VII. Disorder-induced current generation

In this section, we first analyze the upper and lower limits of the linear shape of the envelope curve of the current as a function of disorder strength  $V$  in Fig. 2(c) in the main text, and further explain how, as  $V$  increases, the upper and lower limits of the envelope curve change from being linearly dependent on  $V$  to being independent of  $V$ . To analyze these effects clearly, we first consider a two-site example. The Hamiltonian of the model is  $H_S = -(c_1^\dagger c_2 + h.c.) + \sum_{j=1}^2 V_j c_j^\dagger c_j$ , where the potential  $V_j$  is randomly distributed in  $[-V, V]$ . The on-site loss terms are  $L_j = \sqrt{\gamma}c_j$ , with  $j = 1, 2$ . When  $f_L = f_R = f$ , the current  $J^0$  can be represented as  $J^0 = \Gamma \int \frac{d\omega}{h} f(\omega) \tau_{0,l}(\omega)$  with  $\tau_{0,l} = \text{Tr}[(\mathbf{\Gamma}_L + \mathbf{\Gamma}_R) \mathbf{G}_S^R \mathbf{P} \mathbf{G}_S^R]$  and  $\mathbf{G}_S^R = \frac{1}{\omega - \mathbf{h}_S + i\mathbf{P}}$ . Here  $\mathbf{\Gamma}_L = [\Gamma, 0; 0, 0]$ ,  $\mathbf{\Gamma}_R = [0, 0; 0, \Gamma]$ ,  $\mathbf{h}_S = [V_1, -1; -1, V_2]$  and  $\mathbf{P} = [\gamma, 0; 0, \gamma]$ . After a straightforward calculation, we derive

$$\tau_{0,l}(\omega) = \gamma \frac{\bar{V}_2^2 - \bar{V}_1^2}{(\bar{V}_1 \bar{V}_2 - \bar{\gamma}^2 - 1)^2 + \bar{\gamma}^2 (\bar{V}_1 + \bar{V}_2)^2}, \quad (\text{S49})$$

where the shifted potentials  $\bar{V}_1 = \omega - V_1$  and  $\bar{V}_2 = \omega - V_2$  are randomly distributed in  $[\omega - V, \omega + V]$ , and  $\bar{\gamma} = \gamma + \frac{\Gamma}{2}$ . The envelope curve of  $J^0$  is determined by the maximum value of  $\tau_{0,l}$ , which is difficult to calculate in general. However,

it can be derived in the weak disorder limit (neglecting the  $V_2^2 - V_1^2$  term in the numerator, the denominator satisfies  $(\bar{V}_1 + \bar{V}_2)^2 \sim 4\omega^2$ ,  $\bar{V}_1\bar{V}_2 \sim \omega^2$ ), the current can be approximated by

$$J^0 = \gamma\Gamma \int \frac{d\omega}{h} f(\omega) \frac{2\omega(V_1 - V_2)}{4\omega^2\bar{\gamma}^2 + (\omega^2 - \bar{\gamma}^2 - 1)^2}. \quad (\text{S50})$$

Hence if the potential is symmetric  $V_1 = V_2$ , the current vanishes  $J^0 = 0$ . Conversely, if the potential is the “most” asymmetric  $V_1 = -V_2 = \pm V$ , the current reaches its maximum. The envelope curve is then  $J^0 \sim \pm cV$  with  $c = \int \frac{d\omega}{h} f(\omega) \frac{4\omega\gamma\Gamma}{4\omega^2\bar{\gamma}^2 + (\omega^2 - \bar{\gamma}^2 - 1)^2}$ . This represents the upper and lower limits of the linear envelope, and it can be seen that as the loss strength  $\gamma \rightarrow 0$ ,  $c$  becomes 0, and  $J^0$  also becomes 0.

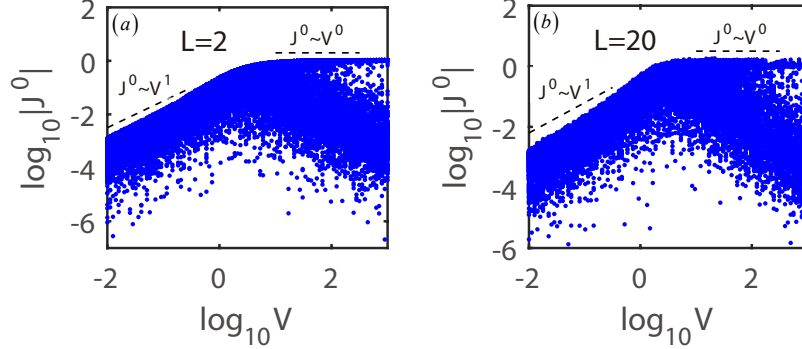


Figure S3: The current  $J^0$  as a function of disorder strength  $V$  in the zero temperature limit. The chemical potentials  $\mu_L = \mu_R = 0.1$ . The system sizes are (a)  $L = 2$  and (b)  $L = 20$ .

In the strong disorder limit, the hopping between two sites can be neglected ( $V_1, V_2 \gg 1$ , where 1 is the hopping strength we chose). We can view the left lead couples to the first site, and the right lead couples to the second site. In this case, Particles can only effectively propagate at the resonance points  $\omega \sim V_1$  and  $\omega \sim V_2$ , and the response rapidly decreases away from these resonance points. Therefore, the main contribution to the transmission function comes from these frequency points, which can be approximated as two peaks of a Lorentzian function. Substitute  $\omega = V_1$  and  $\omega = V_2$  into Eq. (S49) (note:  $\bar{V}_1 = \omega - V_1$  and  $\bar{V}_2 = \omega - V_2$ ), and obtain the coefficients in front of  $\delta(\omega - V_1)$  and  $\delta(\omega - V_2)$  respectively. Combining them gives

$$\tau_{0,l}(\omega) \approx \gamma \frac{(V_1 - V_2)^2}{(1 + \bar{\gamma}^2)^2 + \bar{\gamma}^2(V_1 - V_2)^2} [\delta(\omega - V_1) - \delta(\omega - V_2)]. \quad (\text{S51})$$

Then the current is

$$J^0 = \frac{\gamma\Gamma}{h} [f(V_1) - f(V_2)] \frac{(V_1 - V_2)^2}{(1 + \bar{\gamma}^2)^2 + \bar{\gamma}^2(V_1 - V_2)^2}. \quad (\text{S52})$$

Since  $|f(V_1) - f(V_2)| \leq 1$  and  $\frac{(V_1 - V_2)^2}{(1 + \bar{\gamma}^2)^2 + \bar{\gamma}^2(V_1 - V_2)^2} \leq \frac{4V^2}{(1 + \bar{\gamma}^2)^2 + 4\bar{\gamma}^2V^2} \leq \frac{1}{\bar{\gamma}^2}$ , in the strong disorder limit, the maximum value of  $J^0$  is finite and will not increase indefinitely, and it is no longer dependent on the value of  $V$ . In Fig. S3(a) we show the norm of the current  $|J^0|$  as a function of disorder strength  $V$  in the logarithmic coordinate. We find  $J^0 \sim V$  for small disorder strength, and  $J^0 \sim V^0$  for large disorder strength. Hence as disorder strength  $V$  increases, the current increases linearly and then reach its saturation. Though our analysis are based on the two site example, the behavior is similar for large system size from numerical calculation, as shown in Fig. S3(b).

Next, we consider a model incorporating with spin-orbit coupling (SOC):

$$H = -t_S \sum_{j\sigma} (c_{j+1\sigma}^\dagger c_{j\sigma} + h.c.) + t_{SO} \sum_j (c_{j\uparrow}^\dagger c_{j+1\downarrow} + c_{j\downarrow}^\dagger c_{j+1\uparrow} + h.c.) + \sum_{j\sigma} V_{j\sigma} c_{j\sigma}^\dagger c_{j\sigma}, \quad (\text{S53})$$

where  $t_S$  is the hopping amplitude and  $t_{SO}$  denotes the SOC strength. We first consider the case where only spin-up particles experience the disorder ( $V_{j\downarrow} = 0$ ,  $V_{j\uparrow} \in [-V, V]$ ). When  $t_{SO} = 0$ , spin-up and spin-down particles propagate independently. Consequently, the current  $J_\uparrow^0 \neq 0$ , while  $J_\downarrow^0 = 0$ , due to the inversion symmetry, as illustrated in Fig. S4(a). However, for  $t_{SO} \neq 0$ , the SOC enables spin-flip processes, leading to a finite  $J_\downarrow^0$ , as shown in Fig. S4(b) and

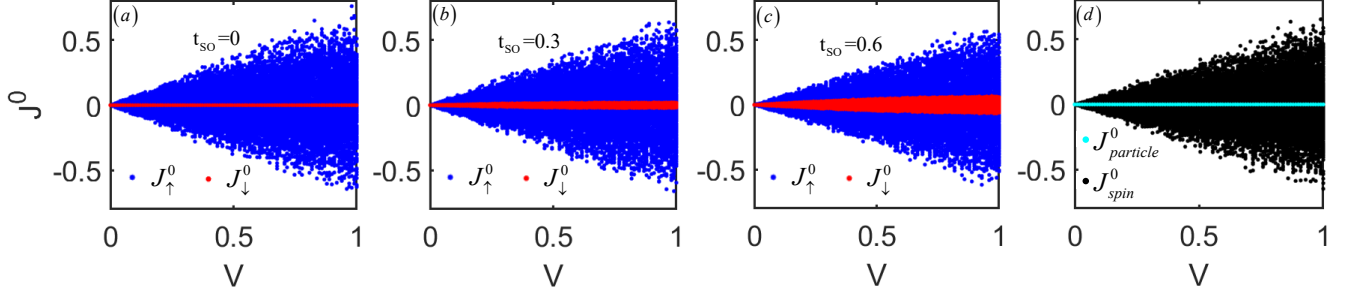


Figure S4: (a)-(c) The current  $J_{\uparrow}^0$  and  $J_{\downarrow}^0$  as a function of disorder strength  $V$  with  $V_{j\downarrow} = 0$ . (d) The particle and spin current as a function of disorder strength  $V$  with  $V_{j\uparrow} = V_{L+1-j\downarrow}$ , the SOC strength  $t_{SO} = 0.3$ . The temperature  $T = 0$ , the chemical potentials  $\mu_L = \mu_R = 0.1$ , and the system size  $L = 10$  are fixed.

(c). The maximum spin-down current increases with  $t_{SO}$ , reflecting the SOC-assisted activation of the otherwise inert spin-down channel.

We then consider another type of spin-dependent disorder with inversion symmetry:  $V_{j\uparrow} = V_{(L+1-j)\downarrow}$  (We note that our following discussion only requires the condition to be satisfied as long as the distributions of  $V_{j\uparrow}$  and  $V_{j\downarrow}$  themselves do not exhibit reflection symmetry, and it is not necessary for  $V_j$  to be disordered). Under this configuration, the spin-up potential at site  $j$  is mirrored by the spin-down potential at site  $L+1-j$ , and the hopping and SOC terms remain invariant under the combined operation of inversion and spin flip (the same phenomenon will occur even  $t_{so} = 0$ ). As a result, the spin-resolved currents satisfy  $J_{\uparrow}^0 = -J_{\downarrow}^0$ . Therefore, the total particle current  $J_{particle}^0 = J_{\uparrow}^0 + J_{\downarrow}^0$  vanishes, while the spin current  $J_{spin}^0 = \frac{1}{2}(J_{\uparrow}^0 - J_{\downarrow}^0)$  is finite, which can be verified from numerical calculations as illustrated in Fig. S4(d).

These findings demonstrate that the combination of spin-dependent disorder and SOC can be harnessed to realize controllable spin currents without net particle transport. Such spin-selective transport behavior has potential applications in the design of spin filters, spin valves, and other spintronic devices. In particular, the ability to generate pure spin currents through disorder engineering and SOC offers a promising route toward low-dissipation information processing. Our results also provide insights for implementing similar mechanisms in experimental platforms such as cold atoms, mesoscopic conductors, and synthetic quantum materials with tunable spin and dissipation control.

The disorder average of  $(J^0)^2$  is

$$\langle (J^0)^2 \rangle = \frac{1}{4V^2} \int_{-V}^V \frac{c^2}{4} (V_1 - V_2)^2 dV_1 dV_2 = \frac{1}{6} c^2 V^2. \quad (\text{S54})$$

It can be shown numerically that this scaling relation  $\langle (J^0)^2 \rangle \sim V^2$  holds for large system size  $N$  (see Fig. 2(d) in the main text).

### VIII. Response current and the Wiedemann-Franz law

In this section, we focus on the response current  $\delta J_1^\lambda$ . In the presence of chemical potential and temperature gradients, the change in currents can be written as

$$\begin{pmatrix} \delta J_1^0 \\ \delta J_1^Q \end{pmatrix} = \begin{pmatrix} L_{11} & L_{12} \\ L_{21} & L_{22} \end{pmatrix} \begin{pmatrix} \frac{\delta\mu}{T} \\ \frac{\delta T}{T^2} \end{pmatrix}, \quad (\text{S55})$$

where  $\delta J_1^Q = \delta J_1^1 - \mu_L \delta J_1^0 - \delta\mu J_0^0$ , and  $\mathbf{L}$  is the Onsager matrix [7, 8]. Then, the electrical conductance  $G$ , the thermal conductance  $K$ , and the Seebeck factor (or thermopower)  $S$  can be expressed as

$$G = \frac{e^2}{T} L_{11}, \quad K = \frac{1}{T^2} \frac{\det |\mathbf{L}|}{L_{11}}, \quad S = \frac{1}{eT} \frac{L_{12}}{L_{11}}. \quad (\text{S56})$$

In the linear response regime, the Fermi function difference is

$$\delta f = f_L - f_R = \frac{\partial f}{\partial T} \delta T + \frac{\partial f}{\partial \mu} \delta \mu = -f'(\omega) \left[ \frac{\omega - \mu}{T} \delta T + \delta \mu \right], \quad (\text{S57})$$

with  $f'(\omega) = \frac{-1}{4k_B T \cosh^2(\frac{\omega-\mu}{2k_B T})}$ . In the zero-temperature limit,  $f'(\omega) \rightarrow -\delta(\omega - \mu)$ , and in the high-temperature limit,  $f'(\omega) \rightarrow \frac{-1}{4k_B T}$ . It is convenient to define the integral

$$I_k = - \int d\omega (\omega - \mu)^k f'(\omega) \tau_1(\omega), \quad (\text{S58})$$

from which we find the Onsager matrix elements are  $L_{11} = \frac{T}{h} I_0$ ,  $L_{12} = L_{21} = \frac{T}{h} I_1$ ,  $L_{22} = \frac{T}{h} I_2$ . Hence, all the response functions in Eq. (S56) can be expressed in terms of  $I_k$ . If  $\tau_1(\omega)$  is a continuous function near the chemical potential  $\mu$ , then in the low-temperature limit, Eq. (S58) can be approximated by

$$I_0 = \tau_1(\mu), \quad I_1 = \frac{\pi^2}{3} (k_B T)^2 \frac{d\tau_1(\mu)}{d\mu}, \quad I_2 = \frac{\pi^2}{3} (k_B T)^2 \tau_1(\mu). \quad (\text{S59})$$

Then the ratio  $\frac{K}{G}$  is given by

$$\frac{K}{G} = \frac{1}{e^2 T} \frac{I_0 I_2 - I_1^2}{I_0^2} = \mathcal{L} T [1 - \frac{\pi^2}{3} (k_B T)^2 (\frac{\tau_1'(\mu)}{\tau_1(\mu)})^2], \quad (\text{S60})$$

where the Lorenz number is  $\mathcal{L} = \frac{\pi^2}{3} (\frac{k_B}{e})^2$ . The Wiedemann-Franz law holds if  $|\frac{\tau_1'(\mu)}{\tau_1(\mu)}| \ll (k_B T)^{-1}$ . In the absence of gain and loss,  $|\frac{\tau_1'(\mu)}{\tau_1(\mu)}|$  becomes very large near the band edge or outside the band, leading to a breakdown of the Wiedemann-Franz law. However, gain and loss smooth the transmission function  $\tau_1(\omega)$ , ensuring that the Wiedemann-Franz law holds across all energy regimes.

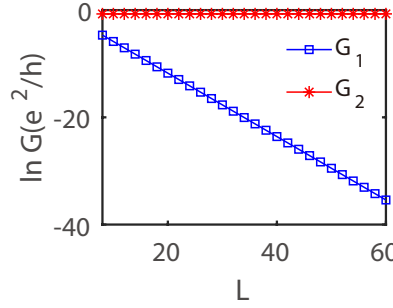


Figure S5: The zero temperature conductance versus system size in the unit of  $e^2/h$ . The parameter  $t_S = 1$ ,  $\mu = 0.1$  and  $\gamma = 0.1$ .

We now consider the size-dependent of conductance. The expression for conductivity at any temperature is:  $G = \frac{e^2}{T} L_{11} = \frac{e^2}{h} \int d\omega \frac{\delta f(\omega)}{\delta \mu} \tau_1(\omega)$ . For convenience, we focus on the zero-temperature limit, such that the conductance is proportional to the transmission function,  $G = \frac{e^2}{h} \tau_1$ . The transmission function  $\tau_1$  can be decomposed into two terms,  $\tau_1 = \tau_{11} + \tau_{12}$ , leading to  $G_1 = \frac{e^2}{h} \tau_{11}$  and  $G_2 = \frac{e^2}{h} \tau_{12}$ , where  $\tau_{11} = \frac{1}{2} \text{Tr}[\Gamma_L \mathbf{G}_S^R \Gamma_R \mathbf{G}_S^A + \Gamma_R \mathbf{G}_S^R \Gamma_L \mathbf{G}_S^A]$  is the direct transmission function between the two leads; and  $\tau_{12} = \text{Tr}[\Gamma_L \mathbf{G}_S^R (\mathbf{P} + \mathbf{Q}) \mathbf{G}_S^A]$  describes the indirect transmission from the left lead, through the reservoirs, and then to the right lead. It can be seen that  $G_2$  arises entirely due to the presence of loss ( $\mathbf{P}$ ) and gain ( $\mathbf{Q}$ ). In the absence of loss and gain, the conductance  $G_2$  vanishes. Moreover, as shown in our work, the Green's function is given by  $(\mathbf{G}_S^R)^{-1} = \omega - \mathbf{h}_S + i\mathbf{P} + i\mathbf{Q} - \tilde{\Sigma}_L^R - \tilde{\Sigma}_L^R$ . Therefore, when loss or gain is introduced into the system, in addition to generating the conductance  $G_2$ , the conductance  $G_1$  is also modified due to the effective change in the system Hamiltonian from  $\mathbf{h}_S$  to  $\mathbf{h}_S - i\mathbf{P} - i\mathbf{Q}$ . Without loss of generality, we take the simplest tight-binding model,  $H_S = -t_S \sum_j (c_j^\dagger c_{j+1} + h.c.)$ , as an example. In the absence of loss and gain, the finite conductance comes from the contacting conductance at the boundary, and the bulk is resistanceless. When adding the particle loss (or gain) at each site  $L_j = \sqrt{\gamma_l} c_j$  ( $L_j = \sqrt{\gamma_g} c_j^\dagger$ ), the particle can scatter to the reservoirs in the bulk and acquire a finite lifetime, hence  $G_1$  will decrease as the system size increases. Then for the conductance  $G_2$ , the particles can also scatter to the reservoir at each site and acquire a finite lifetime. However, the total number of loss (or gain) channels increases with system sizes. Hence the conductance  $G_2$  will be size-independent. Fig. S5 shows the conductance versus system size, it can be observed the Landauer conductance  $G_1$  decays exponentially with increasing  $L$ , while  $G_2$  is almost a constant. As a result, in the limit of a long system, the total conductance approaches a constant value  $G \approx G_2 \neq 0$ , demonstrating that a non-zero conductivity can persist even in the thermodynamic limit.



Eq. (S65) can be rewritten as

$$\begin{cases} \begin{pmatrix} \Delta_{1,j} \\ \Delta_{1,j-1} \end{pmatrix} = \bar{T}_j \bar{T}_{j-1} \cdots \bar{T}_1 \begin{pmatrix} 1 \\ \frac{(\tilde{\Sigma}_L^R)_{11}}{X_{0,1}X_{1,0}} \end{pmatrix}, & 1 \leq j < N, \\ \begin{pmatrix} \Delta_{1,N} \\ \Delta_{1,N-1} \end{pmatrix} = \begin{pmatrix} 1 & -(\tilde{\Sigma}_R^R)_{NN} \\ 0 & 1 \end{pmatrix} \bar{T}_N \bar{T}_{N-1} \cdots \bar{T}_1 \begin{pmatrix} 1 \\ \frac{(\tilde{\Sigma}_L^R)_{11}}{X_{0,1}X_{1,0}} \end{pmatrix}, & j = N. \\ \begin{pmatrix} \Delta_{1,N} \\ \Delta_{2,N} \end{pmatrix} = \begin{pmatrix} 1 & -(\tilde{\Sigma}_L^R)_{11} \\ 0 & 1 \end{pmatrix} \tilde{T}_1 \tilde{T}_2 \cdots \tilde{T}_N \begin{pmatrix} 1 \\ \frac{(\tilde{\Sigma}_R^R)_{NN}}{X_{N,N+1}X_{N+1,N}} \end{pmatrix}, & j = 1, \\ \begin{pmatrix} \Delta_{j,N} \\ \Delta_{j+1,N} \end{pmatrix} = \tilde{T}_j \tilde{T}_{j+1} \cdots \tilde{T}_N \begin{pmatrix} 1 \\ \frac{(\tilde{\Sigma}_R^R)_{NN}}{X_{N,N+1}X_{N+1,N}} \end{pmatrix}, & 1 < j \leq N. \end{cases} \quad (\text{S66})$$

Here, for convenience, we define  $X_{N,N+1} = X_{N,1}$ ,  $X_{N+1,N} = X_{1,N}$ ,  $X_{1,0} = X_{1,N}$  and  $X_{0,1} = X_{N,1}$ .

Substituting Eq. (S63) into Eq. (S61), we obtain

$$\begin{aligned} \tau_{0,l}(\omega) = & 2\gamma_- \Gamma \sum_{j=1}^N [(-t_S - \gamma_-)^{2N-2j} - (-t_S + \gamma_-)^{2N-2j}] \frac{|\Delta_{1,j-1}|^2}{|\Delta_{1,N}|^2} \\ & + 2\gamma_- \Gamma \sum_{j=1}^{N-1} [(-t_S - \gamma_-)^{2N-2j-1} + (-t_S + \gamma_-)^{2N-2j-1}] \text{Im} \frac{\Delta_{1,j} \Delta_{1,j-1}^*}{|\Delta_{1,N}|^2}. \end{aligned} \quad (\text{S67})$$

The transfer matrix (S65) becomes

$$\bar{T} = \tilde{T} = \begin{pmatrix} \omega + 2i\gamma_- & \gamma_-^2 - t_S^2 \\ 1 & 0 \end{pmatrix}. \quad (\text{S68})$$

The eigenvalues are  $\lambda_{\pm} = \frac{\omega + 2i\gamma_- \pm \Delta}{2}$ , with  $\Delta = \sqrt{\omega^2 - 4t^2 + 4i\omega\gamma_-}$ . From Eq. (S66), we get

$$\begin{aligned} \Delta_{1,j} &= \frac{1}{\Delta} (s_{j+1} + \frac{i\Gamma}{2} s_j), & 1 \leq j < N, \\ \Delta_{1,N} &= \frac{1}{\Delta} [s_{N+1} + i\Gamma s_N - \frac{\Gamma^2}{4} s_{N-1}] & j = N, \end{aligned} \quad (\text{S69})$$

where  $s_j = \lambda_+^j - \lambda_-^j$ .

We consider the special case  $t_S = -\gamma_-$  and the low-energy limit  $\omega \ll |t_S|, \gamma_-$ . Up to leading order,  $\lambda_+ = 0$  and  $\lambda_- = -(\omega + 2it)$ , and the transmission function in Eq. (S67) can be simplified to

$$\tau_{0,l}(\omega) = \frac{4\gamma_- \Gamma}{|\Delta_{1,N}|^2} \sum_{j=1}^{N-1} (-2t_S)^{2N-2j-1} \text{Re} \left[ \Delta_{1,j-1} (t_S \Delta_{1,j-1}^* + \frac{i}{2} \Delta_{1,j}^*) \right], \quad (\text{S70})$$

where

$$\begin{aligned} \Delta_{1,0} (t \Delta_{1,0}^* + \frac{i}{2} \Delta_{1,1}^*) &= \frac{\Gamma}{4} + \frac{i\omega}{2}, \\ \Delta_{1,j-1} (t \Delta_{1,j-1}^* + \frac{i}{2} \Delta_{1,j}^*) &= \frac{i\omega}{2} [\omega^2 + \frac{1}{4} (4t_S - \Gamma)^2] \times (\omega^2 + 4t_S^2)^{j-2}, \\ |\Delta_{1,N}|^2 &= [\omega^2 + \frac{1}{4} (4t_S - \Gamma)^2]^2 \times (\omega^2 + 4t_S^2)^{N-2}. \end{aligned} \quad (\text{S71})$$

Substituting Eq. (S71) into Eq. (S70), we obtain

$$\tau_{0,l}(\omega) = \frac{2\gamma_-^2 \Gamma^2}{[\omega^2 + \frac{1}{4} (4t_S - \Gamma)^2]^2} \left(1 + \frac{\omega^2}{4t_S^2}\right)^{2-N} \sim \frac{2e^2 \gamma_-^2 \Gamma^2}{[\omega^2 + \frac{1}{4} (4t_S - \Gamma)^2]^2} e^{-\frac{\omega^2}{4t_S^2} N}. \quad (\text{S72})$$

Similarly, for  $t_S = \gamma_-$ , we can derive

$$\tau_{0,l}(\omega) \sim -\frac{2e^2 \gamma_-^2 \Gamma^2}{[\omega^2 + \frac{1}{4} (4t - \Gamma)^2]^2} e^{-\frac{\omega^2}{4t_S^2} N}. \quad (\text{S73})$$

Though Eq. (S72) and Eq. (S73) are derived for  $|t_S| = |\gamma_-|$ , the scaling  $\tau_{0,l} \sim e^{-\omega^2 N}$  provides a good approximation for  $|t_S| \geq |\gamma_-|$  based on numerical calculations. Then the current at zero temperature is

$$J_0^0 = \int_{-\infty}^{\mu} \frac{d\omega}{h} \tau_{0,l}(\omega) \sim \sqrt{\frac{\pi}{4hN}} [1 + \text{erf}(\mu\sqrt{N})], \quad (\text{S74})$$

where  $\text{erf}(x) = \frac{2}{\sqrt{\pi}} \int_0^x e^{-t^2} dt$  is the error function. The asymptotic expansion of error function is  $\text{erf}(x) \sim 1 - \frac{e^{-x^2}}{\sqrt{\pi x}}$  as  $x \rightarrow \infty$ , and  $\text{erf}(x) \sim -1 - \frac{e^{-x^2}}{\sqrt{\pi x}}$  as  $x \rightarrow -\infty$ . Hence, in the thermodynamic limit  $N \rightarrow \infty$ , we obtain  $J_0^0 \sim N^{-\frac{1}{2}}$  for  $\mu \geq 0$ , and  $J_0^0 \sim \frac{e^{-N}}{N}$  for  $\mu < 0$ . Therefore, the current corresponding to the skin effect decreases as the size increases and vanishes as the size tends to infinity.

---

\* Corresponding author: wangyc3@sustech.edu.cn

- [1] R. Citro, F. Mancini, *Out-of-equilibrium physics of correlated electron systems* (Springer, 2018).
- [2] C. A. Brasil, F. F. Fanchini and R. J. Napolitano, A simple derivation of the Lindblad equation, *Rev. Bras. Ensino Fis.* **35**, 1 (2013).
- [3] K. Yamamoto, N. Hatano, Thermodynamics of the mesoscopic thermoelectric heat engine beyond the linear-response regime, *Phys. Rev. E* **92**, 042165 (2015).
- [4] L. M. Sieberer, M. Buchhold and S. Diehl, Keldysh field theory for driven open quantum systems, *Rep. Prog. Phys.* **79**, 096001 (2016).
- [5] F. Thompson, A. Kamenev, Field theory of many-body Lindbladian dynamics, *Annals of Physics*, **455**, 169385 (2023).
- [6] Y. Meir, N. S. Wingreen, Landauer formula for the current through an interacting electron region, *Phys. Rev. Lett.* **68**, 2512 (1992).
- [7] P. N. Butcher, Thermal and electrical transport formalism for electronic microstructures with many terminals, *J. Phys.: Condens. Matter* **2**, 4869 (1990).
- [8] C. Chiaracane, A. Purkayastha, M. T. Mitchison, and J. Goold, Dephasing-enhanced performance in quasiperiodic thermal machines, *Phys. Rev. B* **105**, 134203 (2022); C. Chiaracane, M. T. Mitchison, A. Purkayastha, G. Haack, and J. Goold, Quasiperiodic quantum heat engines with a mobility edge, *Phys. Rev. Res.* **2**, 013093 (2020).
- [9] D. A. Lavis, B. W. Southern, The inverse of a symmetric banded toeplitz matrix, *Rep. Math. Phys.* **39**, 137 (1997).
- [10] M. Saha, B. K. Agarwalla, M. Kulkarni, A. Purkayastha, Universal Subdiffusive Behavior at Band Edges from Transfer Matrix Exceptional Points, *Phys. Rev. Lett.* **130**, 187101 (2023).